AN ABSTRACT OF THE THESIS OF

Austin Thody for the degree of Master of Science in Nuclear Engineering presented on January 5, 2018.

Title: Irradiation Capsule Development for Composite Fuels for Nuclear Thermal Propulsion.

Abstract approved:

_____

Andrew C. Klein

Nuclear Thermal Rocket (NTR) designs have recently seen renewed interest due to superior thermal efficiencies and a renewed desire for space exploration. This has resulted in improved NTR fuel designs that have unique properties that require investigation and testing in order to be more safely designed and operated.

Oak Ridge National Laboratory (ORNL) has recently recaptured the “composite” fuel form developed in the Rover/Nuclear Engine for Rocket Vehicle Application (NERVA) Nuclear Thermal Propulsion Programs of the 1960s and 1970s. These elements are now being tested thermally. However, an important aspect of their successful demonstration is irradiation in relevant environments. This project, presents an examination of potential capsule designs that could be used in the examination of composite NTR fuels in test reactors.

Irradiation Capsule Development for Composite Fuels for Nuclear Thermal Propulsion

by
Austin Thody

A THESIS

submitted to

Oregon State University

in partial fulfillment of
the requirements for the
degree of

Master of Science

Presented January 5, 2018
Commencement June 2018

Master of Science thesis of Austin Thody presented on January 5, 2018

APPROVED:

Major Professor, representing Nuclear Engineering

Head of the School of Nuclear Science and Engineering

Dean of the Graduate School

I understand that my thesis will become part of the permanent collection of Oregon State University libraries. My signature below authorizes release of my thesis to any reader upon request.

Austin Thody, Author

ACKNOWLEDGEMENTS

There are many people I would like to thank for the completion of this project. I would like to thank Dr. Andrew Klein for being a great advisor over the last couple of years and for his assistance and guidance on this project.

I would like to thank everyone involved with assisting me in my understanding and education of MCNP. Thank you, Dr. Todd Palmer, for initially teaching me how to use MCNP. Thank you, Robert Schickler, for helping me understand to the OSU MCNP TRIGA model, as well as teaching me about the MCNP multiplier cards. Thank you, Dr. Haori Yang, for helping me work though creating a flux profile and in general the understanding of MCNP. This would not have been possible without each of you.

I would like to thank my committee (Dr. Brian Woods, Dr. Leah Minc, Dr. Andrew Klein and Dr. Wade Marcum) for their help.

I would like to thank those of you who have helped me reach this point in my education. The many educators who have supported me throughout all this time. From the teachers who first helped me learn to read, to the instructors teaching me physics in high school, and now finishing my master's degree. Reaching this point has not been easy, but through your support it has been possible, thank you.

Finally, I would like to thank my friends and family for always being there and supporting me through this long and difficult process. Especially my mom, you have been my biggest supporter and have always been there for me. There is nothing more that I could have asked for from you. This has been a very stressful endeavor, but I thank all of you for supporting me throughout the process.

TABLE OF CONTENTS

LIST OF FIGURES

Figure Page

LIST OF TABLES

Table Page

Irradiation Capsule Design for Composite Fuels for Nuclear Thermal Propulsion

1. Introduction

Coated particle graphite fuels, especially for nuclear thermal propulsion in space applications were studied extensively during the Rover/NERVA programs from 1955 to 1975. Due to their greater experience base, ease of fabrication, and lower thermal neutron absorption cross sections, these are a leading fuel technology for nuclear thermal propulsion [1]. In addition, coated particle fuels are currently being developed and studied for commercial high-temperature reactor applications [2]. Composite fuels were developed as a "drop-in" replacement for coated particle graphite fuels as seen in Figure 1-1. In composite fuels, carbide-based ceramic fuel is mixed within a graphite matrix.

Composite fuels were tested under representative reactor conditions in the Nuclear Furnace-1 (NF-1) in July 1972 [3]. The NF-1 reactor was designed for fuel testing and was not designed or utilized as a standalone nuclear thermal propulsion (NTP) reactor. In addition, during this program Westinghouse performed full-length, externally-heated tests on the prototype test material at approximately 2700 K (but not in an irradiation environment). However, the program was cancelled prior to the planned testing of the composite fuel form in an NTP reactor. [19]

Follow-up reactor concept development efforts incorporated zirconium hydride tie tubes for additional neutron moderation in the composite cores. This allowed for smaller reactor cores, such as the Small Nuclear Rocket Engine (SNRE) [4]. This concept was designed to produce 16,400 lbs of thrust at a specific impulse (Isp) of approximately 900 Isp. Though a great deal of engineering effort went into the SNRE as seen in Figure 1-2, the system was never built, tested, or operated.

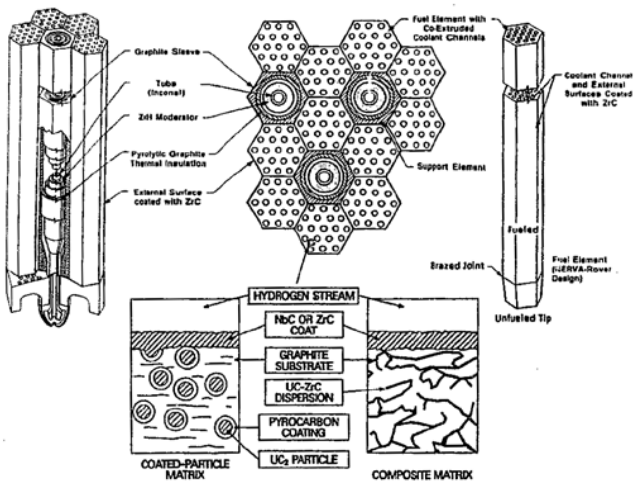

Figure 1-1 Schematic of NERVA Reactors [2].

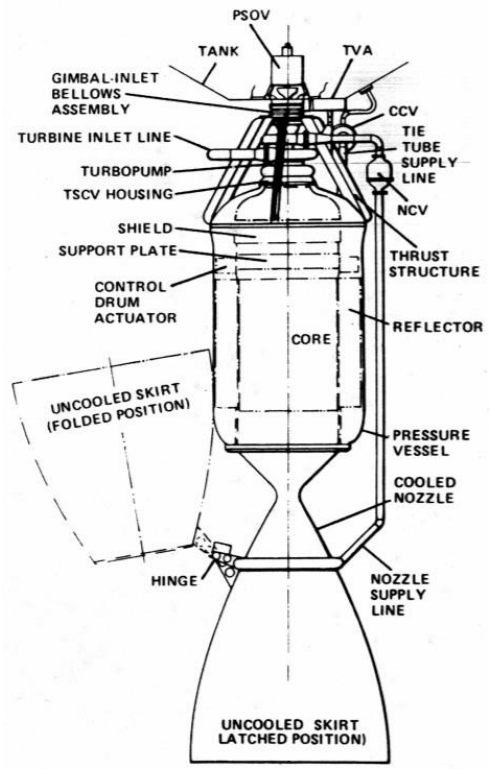

Figure 1-2 Schematic of the Small Nuclear Rocket Engine [2].

Fuel testing during the Rover/NERVA programs identified issues with the protective zirconium carbide (ZrC) coatings, which were used on coolant channels and the exterior of the fuel elements. The issue of the cracking ZrC coating in some of the inner coolant channels of the coated particle graphite fuel elements was never fully examined

or understood [19]. Composite fuels have a higher thermal expansion coefficient than coated particle graphite fuels. The NF-1 composite fuel irradiation tests also identified cracking of the protective coating and within the composite fuel matrix of some elements under those test conditions. Alternative coating options (e.g., use of multiple later coatings) are being pursued to mitigate the coating cracking issue but have not been verified by test.

1.1. Objective

Nuclear Thermal Rocket (NTR) designs have received renewed interest due to their superior thermal efficiencies and a rehabilitated desire for space exploration. This has resulted in improved NTR fuel designs that have unique properties that require investigation and testing in order to be more safely designed and operated.

Oak Ridge National Laboratory (ORNL) has recently recaptured the “composite” fuel form developed in the Rover/Nuclear Engine for Rocket Vehicle Application (NERVA) Nuclear Thermal Propulsion Programs of the 1960s and 1970s [2]. The NERVA fuel elements are now being tested thermally. However, an important aspect of their successful demonstration is irradiation under relevant environments. This project, presents an examination of a few potential capsule designs that could be used in the examination of composite NTR fuels in test reactors.

1.2. Purpose

This study yields a number of significant contributions to the body of knowledge related to NTR fuel testing. First, the results will provide important insights on the capsule-fuel interaction when in the presence of neutrons. Second, the project will provide a high-quality simulation of an irritated capsule and develops a detailed design for irradiating NTR fuel and surrogate fuel materials. Third, it allows for newly developed fuel to be tested in reactor facilities before progressing in the design process. These contributions align with the sought-after development of a nuclear thermal

propulsion system by supporting the development and testing of potential designs. It will also provide assistance for testing current NERVA based fuel designs. This report will present three different capsule designs for three different reactor types. The first capsule design for testing surrogate fuel samples and analyzing neutron damage will be for irradiations in the Oregon State Training, Research, Isotopes, General Atomics (TRIGA) reactor. The second capsule is designed for the High Flux Isotope Reactor (HFIR) at Oak Ridge National Laboratory. This reactor provides a high thermal and cold neutron flux and will be capable of analyzing long term neutron irradiation damage and potential radiation heating. The third and final capsule design is intended for the Advance Test Reactor (ATR) at the Idaho National Laboratory. This reactor has previous experience with testing advanced fuel designs and materials and should be capable of handling a depleted or low enriched uranium test sample. These three capsule designs are being presented in this report for potential future testing.

1.3. Document Overview

This thesis is organized as follows. Chapter 1 is the introduction and describes the motivation of the topic under discussion along with a general logic to the study methodology. Chapter 2 is the literature review and this section provides a review of the available literature on the subject and its relevance to the study. Chapter 3 is the methods section and is a description of the methods used to characterize the reactor capsule design and the use of the Monte Carly neutron transport computer code MCNP [10]. Chapter 4 presents the results of the MCNP analysis and the important simulated results obtained from the study. Chapter 5 provides a discussion of the results obtained in the study. Chapter 6 is used to draw the conclusions of this study and also provides recommendations for future improvements to the modeling and testing of the composite NTR fuels. This study concludes with a list of references and appendices containing additional details about the analysis conducted.

2. Literature Review

This chapter provides a survey of existing, publicly available literature with respect to test reactors capsule designs used for fuel experiments and the use of MCNP and MCNP tally multiplier cards for the simulation of NTR and reactor cores.

2.1. Space Nuclear

There has recently been a revived interest in the use of nuclear fission power for use in space. Radioisotope power has been an important source of energy for space related missions since 1961 [23]. Plutonium-238 has become a vital power source for deep space missions. However, fission reactor power sources have mainly been used by Russia over the last 30 years. The USA has only flown one of these types of reactors the SNAP-10A (System for Nuclear Auxiliary Power) in 1965 [23]. From 1959-73 there was a US nuclear rocket program – Nuclear Engine for Rocket Vehicle Applications (NERVA) which was focused on nuclear power replacing chemical rockets for the latter stages of launches. The NERVA project used a graphite core reactors heating liquid hydrogen which was vaporized and expelled through a nozzle creating propulsion. Around 20 different designs were tested at the Nevada test site and produced a large amount of thrust comparable to shuttle launch systems. After these tests most, nuclear rocket designs have focused on space propulsion not launches.

The successor to the NERVA program of the 1960's is the Space Nuclear Thermal Propulsion (SNTP) program. The SNTP was an effort to develop an advanced nuclear thermal rocket design for the United States that had the potential to be twice as efficient as conventional chemical rockets. The SNTP program developed nuclear engines over a 5-year period and was well along the path of success, when in 1992 changing national priorities and security requirements resulted in the termination of the program. The SNTP program consisted of three phases. Phase I ran from November 1987 through September 1989, the objective of this phase was to verify the feasibility of the Particle Bed Reactor (PBR) as the propulsion energy source for the upper stage of a ground-based Boost Phase Intercept (BPI) vehicle. Phase II started under the control of the

Strategic Defense Initiative Organization but was transfer to the US Air Force in 1991. The goal of Phase II was to perform a ground demonstration of a PBR engine. It was planned that a flight demonstration would be conducted in Phase III of the program. The program was cancelled in 1994, prior to the end of Phase II. The flight test of the SNTP system in Phase III was never performed [19]. Figure 2.1-1 SNTP Program Schedule [19]Figure 2.1-1 bellow details the schedule for the SNTP program and includes the progression of the project.

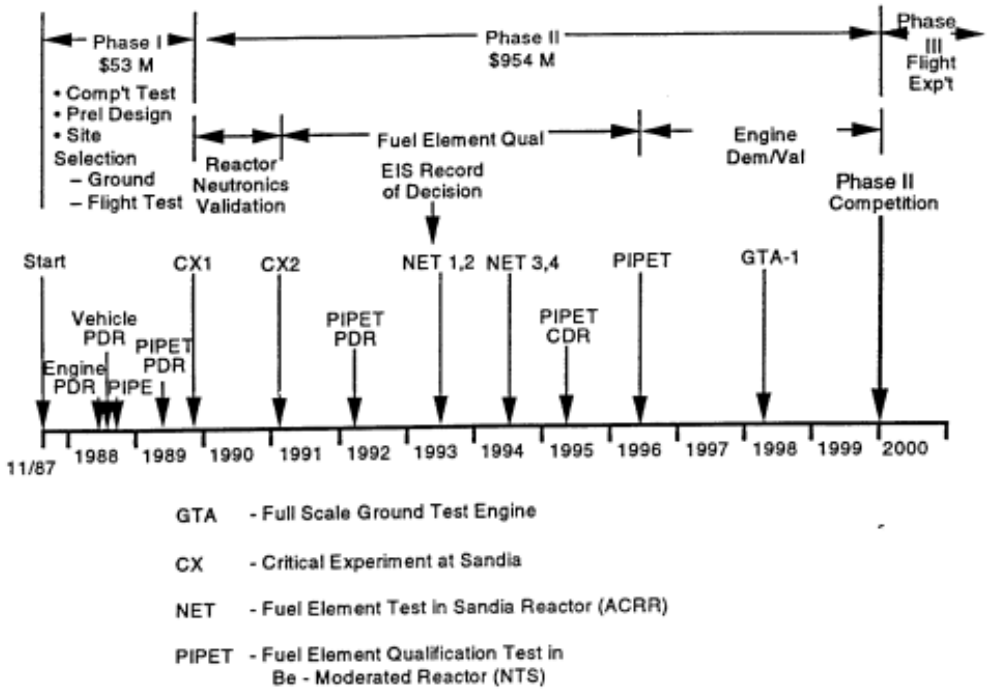

Figure 2.1-1 SNTP Program Schedule [19]

As mentioned in section 1, in the early 1990's thermal testing for NTR fuel was performed for temperatures up to 2700 K [19]. This report detailed several different designs and tests that had been performed during the space nuclear thermal propulsion program. The UC-ZrC coated fuel sample tested during this era can be seen in Figure 2.1-2. However, a serious issue involving the cracking of the ZrC coating on regions of coated particle graphite fuel elements was never fully examined or understood. Due to a lack of funding the program was cancelled prior to the planned testing of the composite fuel in a neutron rich environment.

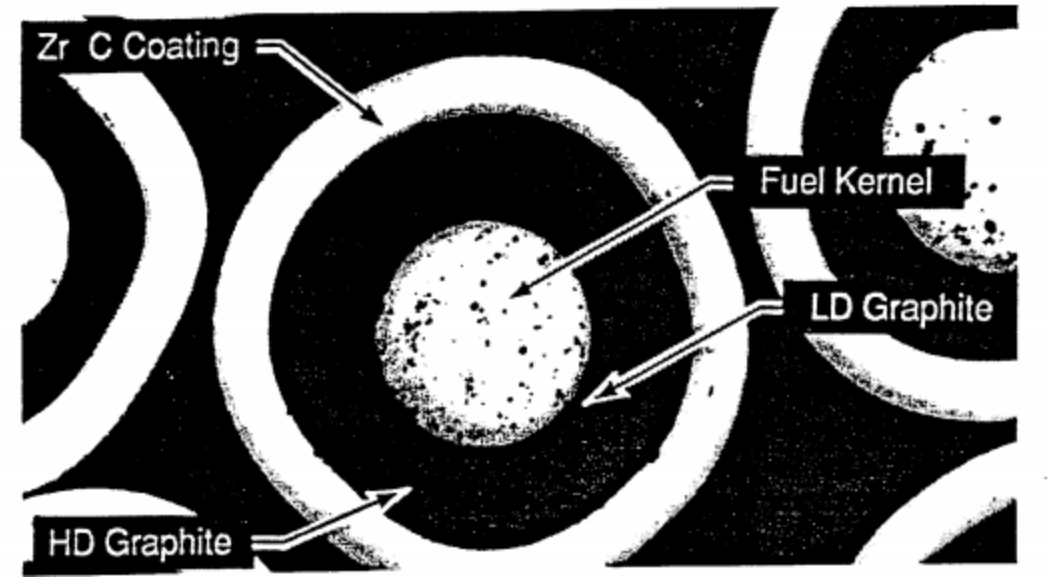

Figure 2.1-2 A Baseline Fuel Particle UC2 with ZrC Coating [19]

In order to proceed with testing the fuel in a neutron rich environment, a capsule design that can survive the high temperatures generated by NRT fuel needs to be developed. In 2010, two experiments, JP30 and JP31 were designed for testing various stainless-steel specimens in the High Flux Isotope reactor [17]. The designs of these capsules can be seen in Figure 2.1-3. These experiments were designed to irradiate F82H specimens of various sizes in the flux trap of HFIR at a temperature range of 300 to 650 °C. The major change for the JP30/31 designs and previous designs is that the maximum temperature the JP30/31 is 650°C compared to the previous maximum of 500°C. The test samples were contained within a holder of either DISPAL (dispersion-strengthened aluminum) or a vanadium alloy (V-4Cr4Ti) with an outer container of Al-6061. Helium is used as the fill gas inside the experiment. The samples temperature is controlled by the size of the gap between the holder and capsule. This 2010 report summarizes the design and thermal test results for the JP30 and JP31 capsule designs. However, these capsule designs do not involve the irradiation of active fuel.

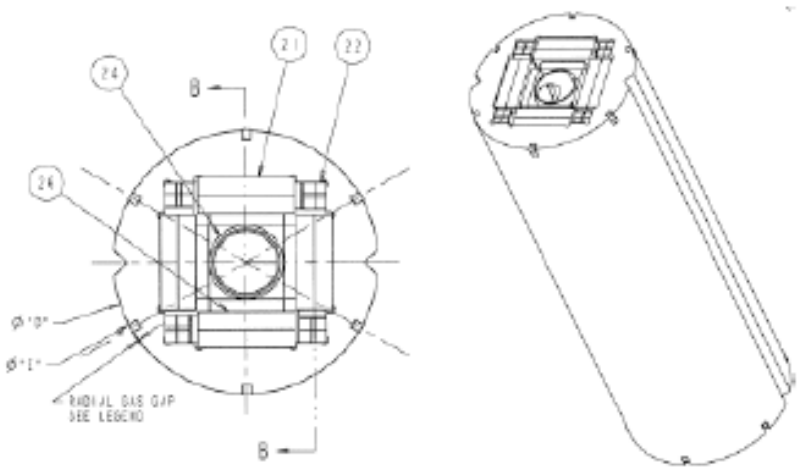

Figure 2.1-3 Specimen Layout for the SSJ3 regions [17].

The Advanced Test Reactor (ATR) does have experience in testing and irradiating active fuels samples. In 1995, mixed oxide fuels testing in the advance test reactor to support plutonium disposition [16] was published with support from Idaho National Engineering Laboratory. This publication lays the ground work for testing mixed oxide fuel in the advanced test reactor and the implications it could have on reducing the weapons-grade plutonium stock pile. This report also includes a detailed description of the ATR core configuration and the normalized flux profile the sample would be exposed to. Finally, the capsule design used for containing and testing the mixed oxide fuel is described in detail. This article also addresses other significant issues with inserting enriched fuel into a test reactor. This is a significant study for all future active fuel testing experiments and simulations. However, this experiment is only looking at MOX fuel inside the ATR reactor and does not deal with LEU fuel for NTR's or with irradiating active fuel in other facilities.

2.2. MCNP

In 2012, the OSU TRIGA MCNP model was updated to represent the newly converted LEU fuel and the resulting flux profile in the core [21]. The new LEU core Monte Carlo N-particle (MCNP) model was compared to the previous HEU FLIP core model. The MCNP model was also compared to experimental data taken from the LS, the ICIT, the CLICIT, the Rabbit, and the TC. The OSTR facilities neutron spectrum was re-

characterized using theoretical simulation (MCNP) and provides corrected neutron spectra through use of the STAY'SL code and experimental data collection. This provides an excellent modeling tool for analyzing theoretical neutron interaction inside the OSU TRIGA core. However, it does not provide a capsule design or a test scenario for an LEU test sample. Thought the multiplier cards used in this TRIGA core model can also be used and applied to other test scenarios.

In 2012, Brad Appel of Texas A&M publish the thesis titled Multiphysics Design and Simulation of a Tungsten-Cermet Nuclear Thermal Rocket Design [22]. This publication includes a complete MCNP input deck for a tungsten cermet design and the multiplier card used to model the design at full power. This publication details the simulated thermal properties of the model as well as the core configuration such as coolant channel size, thermal meshing, and simulated optimal design parameters for this type of core configuration. However, this model does simulate a HEU CERMET core model instead of a composite core model and it is the entire core instead of a small-scale fuel sample being tested inside a reactor. However, it does provide a set of simulation data which can be used to guide materials research and sample fuel element testing programs in addition to best practices for NTR fuel modeling. Though this provides an example of modeling NTR fuel at full thermal power in MCNP.

3. Methods

This section discusses the methods used to calculate the theoretical neutron spectrum that the capsule would be exposed to in a test reactor configuration and determining the resulting thermal energy released by the fuel which will need to be removed, and the potential resulting effects on the capsule. This study is broken into two sections: the first section examines the neutronics calculations and the simulated results from Monte Carlo N-Particle Transport Code (MCNP). The second section evaluates the thermal calculations based off the results from the neutronics calculations.

3.1. Neutronics Calculations Using MCNP

MCNP is a powerful computing tool that uses a Monte Carlo method to determine parameters pertaining to nuclear reactions in a region of defined material composition. The Monte Carlo method is a computational algorithm that relies on random sampling and large samples sample sizes to achieve a numerical result. By using the laws of large numbers, the Monte Carlo method is able to make an accurate estimate on the correct result. However, because of the random nature of the simulation there will always be an associated error with these kinds of calculations. MCNP uses four input parameters, the geometric description of the model, the material description of the structures, the description of a source, and the desired output variables.

The geometric and material properties of the structures must be defined in the input deck that models the desired system. In this case, the desired system is the capsule containing the test fuel and any surrounding structures. This involves defining the surfaces, cells, and materials of the system and these may be modeled in a variety of ways using inputs defined in the MCNP Manual [11]. A number of surfaces must be created to properly define the modeled structure and properly discretize the volume. The specific material desired for every volume utilized in the model must be described based on its atomic makeup. Cells are the combination of the surfaces and material inputs to describe the desired 3-dimensional structures. A radiation source must be defined in order to model the nuclear reactions using the Monte Carlo simulation, in this case a neutron source.

The desired output data from the MCNP simulation must be determined and evaluated. MCNP is capable of many different applications such as dose measurement and calculating criticality, but in this case, it will be used to determine the magnitude of the neutron flux, the neutron material interaction rates, and heat/power generated in those materials. The resulting simulated neutron flux values can be tabulated in specific regions of the model using tally cards. There are several different types of tally cards available in MCNP. The tallies used for this thesis, and the resulting manipulation of these tallies, are defined in section 3.2.

There is a total of 12 MCNP input files referenced by this thesis. The first three cases use the OSU TRIGA reactor in an MCNP model with the capsule simulated in the B1 In-Core Irradiation Tube (ICIT) configuration seen in Figure 3.1-1. The OSU TRIGA MCNP design simulates the 1 MW core configuration, the active fuels and test samples, as well as the surrounding shielding and structure of the TRIGA facility.

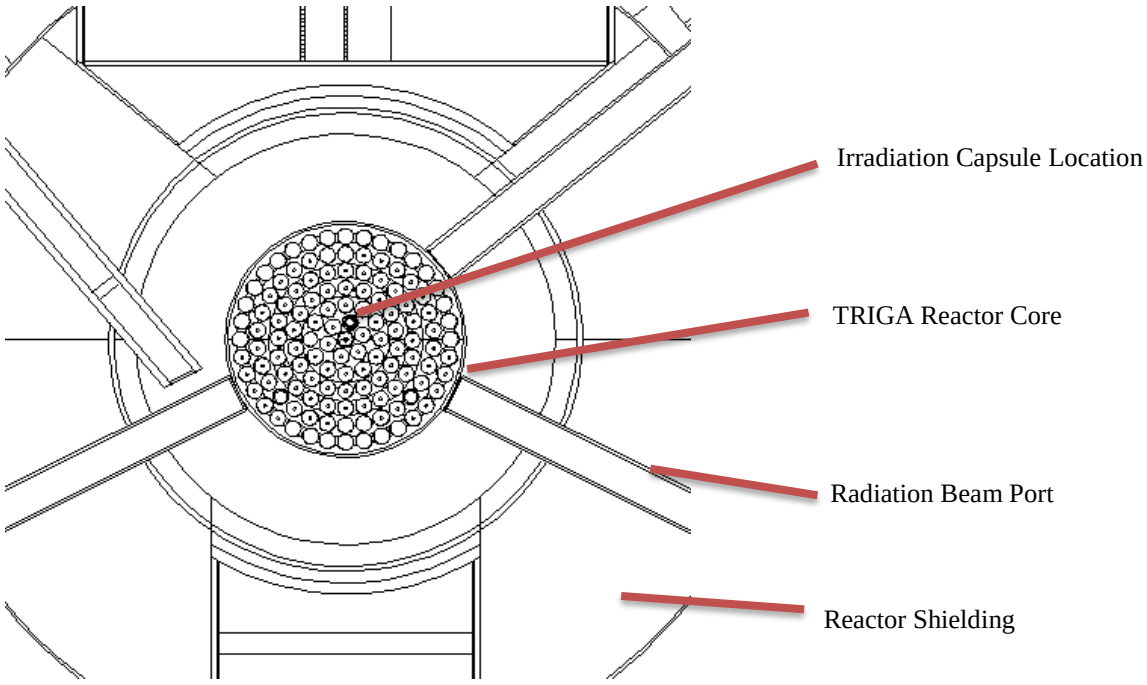

Figure 3.1-1 Top View of the OSU TRIGA Core with Simulated Capsule

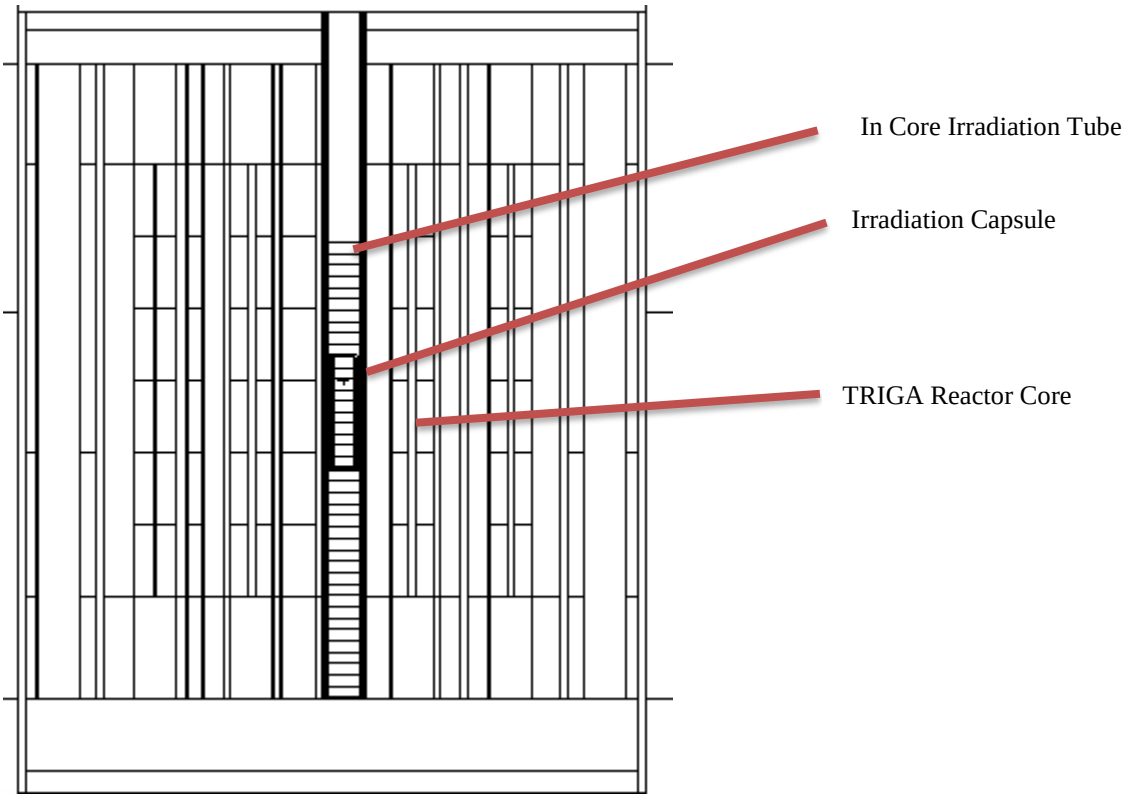

Figure 3.1-2 Side View of TRIGA Core with Simulated Capsule

The first MCNP simulation uses a surrogate fuel of hafnium carbide and zirconium carbide (HfC-ZrC), the second case uses depleted uranium carbide and zirconium carbide (DUC-ZrC) fuel, and the last case uses 19.9% enriched uranium carbide and zirconium carbide (UC-ZrC). The TRIGA capsule design is based off of Figure 3.1-3 with an assumed uniform capsule thickness of 0.143 cm and constructed of aluminum. The test sample has a length of 9.67 cm and a radius of 0.9 cm. The modeled sample is divided into 10 equal size sections along the Z axis.

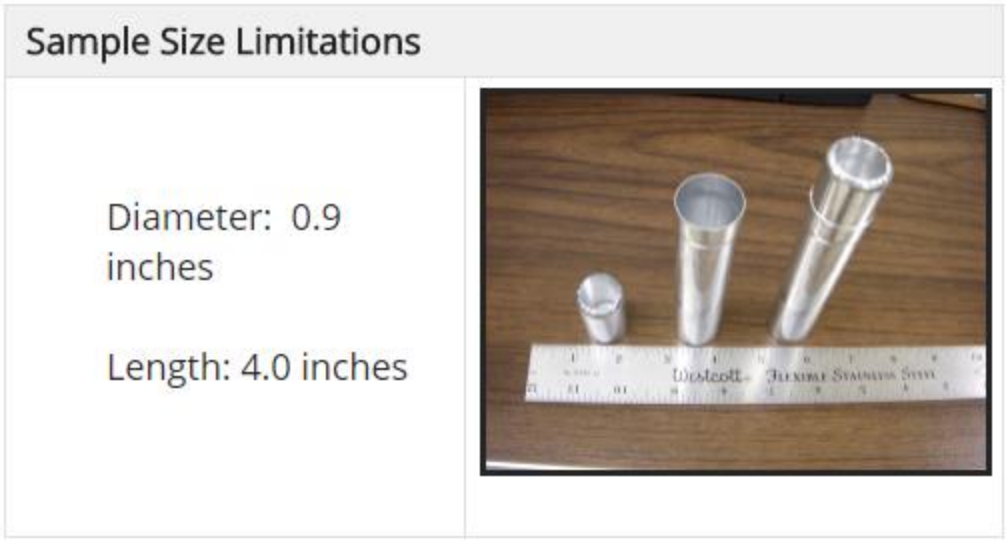

Figure 3.1-3 Encapsulation Limitations OSU TRIGA Reactor [5].

The next three cases use the same fuel loading scenarios as before (HfC-ZrC), (DUC-ZrC), and (UC-ZrC), but uses the predicted ICIT TRIGA flux from reference [5] as shown in Figure 3.1-4. This flux profile is used as a surface source on a cylinder of radius 4.3 cm surrounded by a sphere of water around the capsule as seen in Figure 3.1-5. This should provide a good comparison of modeling the entire core versus just modeling the flux around the capsule. The capsule in Figure 3.1-5 represents the TRIGA capsule submerged in water with a surrounding surface flux. The corresponding cell numbers in Figure 3.1-5 represent different volumes inside of the simulation. Volumes 3-12 represent the test sample broken up into 10 smaller segments.

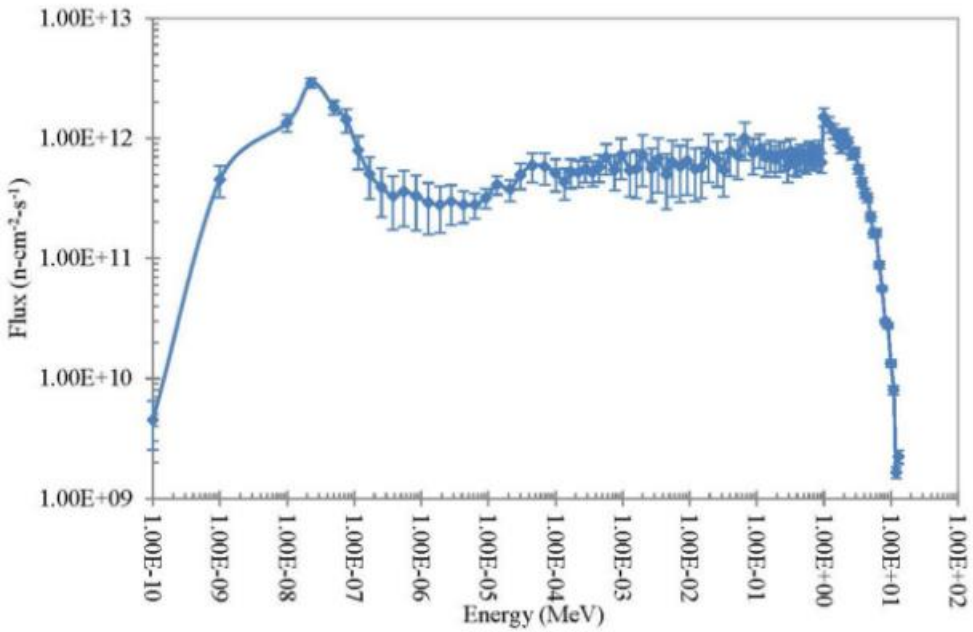

Figure 3.1-4 OSU TRIGA Reactor ICIT Flux [5].

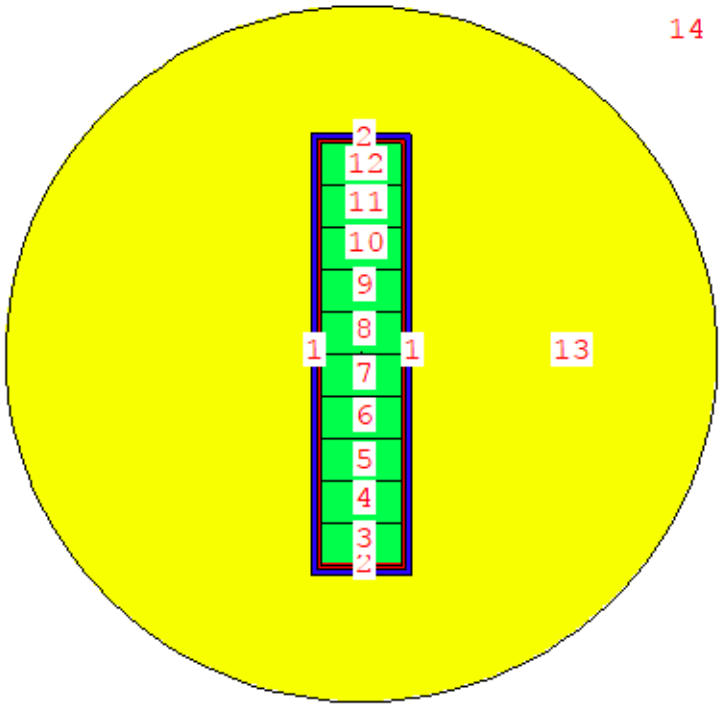

Figure 3.1-5 Simulated Capsule Inside a Sphere of Water

For simulating an environment in MCNP similar to the HFIR core, the neutron flux from reference [6] shown in Figure 3.1-6, was modeled in a similar fashion to the TRIGA capsule with a surrounding water sphere with an inward facing neutron flux on a cylindrical surface with a radius of 6 cm. The flux profile was modeled in this way in order to make an accurate comparison to the full core model by allowing the capsule to be surrounded by the flux spectrum. The capsule was assumed to be in position 4 of the HFIR core and the thermal and fast flux counts were broken into 10 and 20 smaller energy groups respectively. This allows the neutron spectrum to be released in a spectrum of energies and moderated by the water before reaching the test capsule.

Neutron Flux ($N/cm^2/sec$)

Position	Thermal Flux <0.4 eV	Fast Flux >0.183 MeV
1	1.7E+15	7.9E+14
2	2.1E+15	1.0E+15
3	2.4E+15	1.2E+15
4	2.5E+15	1.2E+15
5	2.4E+15	1.2E+15
6	2.1E+15	1.0E+15
7	1.7E+15	7.9E+14
8	1.1E+15	5.1E+14

Figure 3.1-6 HFIR Neutron Flux [6].

The capsule design for the HFIR MCNP simulation is based off of the information provided by reference [6], as seen in Figure 3.1-7. The capsule design matches the dimensions of Figure 3.1-7 with a height of 2.56 inches and inner and outer diameter of .437 and .255 inches. The capsule is modeled as the same aluminum capsule material as the TRIGA capsule. The test samples simulated inside the HFIR capsule are the same

three test samples as the TRIGA capsule model (HfC-ZrC), (DUC-ZrC), and (UC-ZrC) using the dimension of the HFIR model.

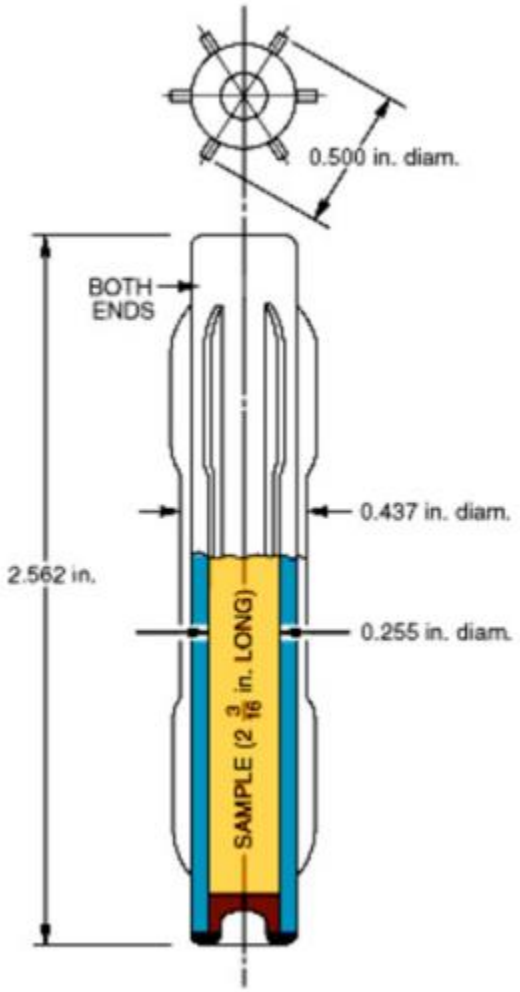

Figure 3.1-7 HFIR Hydraulic Tube Dimensions [6].

The final three MCNP simulations model an environment inside an ATR. The simulated neutron flux is from reference [7] and can be seen in Figure 3.1-8. Unlike the other simulations the thermal power for ATR is simulated at 22 MW instead of the full power of 250 MW in order to more accurately match the flux profile in figure [7]. The flux profile was broken up into a fast and thermal spectrum of 10 groups each to

ensure that the neutrons are not monoenergetic and produce a more accurate spectrum. The flux was modeled as a cylinder on the z axis with a radius of 6 cm and a height of 18 cm with an inward facing flux profile. Similar to the TRIGA model, it is also surrounded by a sphere of water. The capsule was assumed to be without the CD-shroud and the thermal and fast fluxes were simulated in MCNP.

	Thermal neutron flux (E < 0.625 eV) n/cm^2-sec	Fast neutron flux (E > 1.0 MeV) n/cm^2-sec
With CD-shroud	8.46E+12	9.31E+13
Without CD-shroud	3.71E+14	9.39E+13
Ratio	2.28%	99.14%
Note: the flux tallies are normalized to a E-lobe power of 22 MW.		

Figure 3.1-8 ATR Flux Profile [7].

The capsule design for the ATR MCNP simulation is based on the information provided by reference [7] seen in Figure 3.1-9. This capsule design was originally used for testing MOX fuel but should be sufficient for testing low enriched uranium NTR fuel. The capsule design matches the dimensioned described in Figure 3.1-9 with a height of 9.594 inches and an active fuel section of 6.0 inches, and an inner diameter of .322 inches, the test fuel sample has an outer diameter of .327 inches. The ATR capsule uses the same materials defined in Figure 3.1-9 (Zircaloy and stainless-steel cladding). The material simulated inside the ATR capsule are the same three test samples as the TRIGA capsule model (HfC-ZrC), (DUC-ZrC), and (UC-ZrC) using the dimension in Figure 3.1-9.

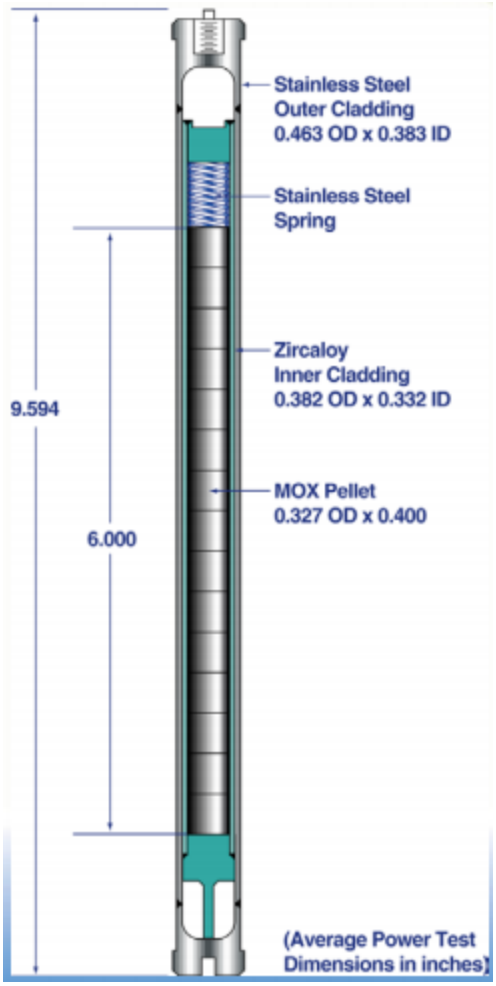

Figure 3.1-9 ATR Capsule Dimensions [7].

3.2. Thermal Calculations

The amount of deposited energy released per fission (Q-value) for each particle is determined from the calculations performed by MCNP6 based on the capsule models described in Section 3.1. The F6 and F7 tallies in the MCNP6 simulation are used to estimate the heating rate from neutrons, fission products, betas, prompt photons, and capture photons. The F6:n tally provides heating rate values from neutrons and fission products and the F7 tally provides heating rates due to production of fission products, neutrons, and prompt photons. The F7 tally also assumes that all the heat produced from the fission products, neutrons, and prompt photons are deposited locally. Each of the tallies provides the heating rates due to contributions from different particles, the

equations from reference [9] show the relationship between the MCNP tallies and the heating rates.

$$q_{F6:n} = q_{fp} + q_n \quad \text{Equation 3.2-1}$$

$$q_{F6:p} = q_{\gamma P} + q_{\gamma c} \quad \text{Equation 3.2-2}$$

$$q_{F7:n} = \left(q_{fP} + q_n + q_{\gamma P}\right) \quad \text{Equation 3.2-3}$$

The variables are defined as:

$q_{F6:n}$ = heating value calculated from MCNP6 using *F6:n* tally (MeV/g-fission neutron)

$q_{F6:p}$ = heating value calculated from MCNP6 using *F6:p* tally (MeV/g-fission neutron)

$q_{F7:n}$= heating value calculated from MCNP6 using *F7* tally (MeV/g-fission neutron)

q_{fP} = energy released by fission products (MeV/g-fission neutron)

$q_{\gamma P}$ = energy released by prompt gammas (MeV/g-fission neutron)

$q_{\gamma c}$ = energy released by capture gammas (MeV/g-fission neutron)

q_n = energy released by neutrons (MeV/g-fission neutron)

After substituting Equation (3.2-1) into Equation (3.2-3), Equation (3.2-3) can be rewritten as:

$$q_{\gamma P} = q_{F7:n} - q_{F6:n} \quad \text{Equation 3.2-4}$$

Equation (3.2-2) can be rewritten as:

$$q_{\gamma c} = q_{F6:n} - q_{\gamma P} \quad \text{Equation 3.2-5}$$

Finally, the Q-values (in MeV/fission) can be found using:

$$Q_{fp} + Q_n = v \sum_{i=1}^{i=cells} \left(\frac{q_{F6:n}^{i}}{K_{eff}} * m_i\right) \quad \text{Equation 3.2-6}$$

$$Q_{\gamma p} = v \sum_{i=1}^{i=cells} \left(\frac{q_{F7:n}^{i}}{K_{eff}} * m_i\right) - v \sum_{i=1}^{i=cells} \left(\frac{q_{F6:n}^{i}}{K_{eff}} * m_i\right) \quad \text{Equation 3.2-7}$$

$$Q_{\gamma c} = v \sum_{i=1}^{i=cells} \left(\frac{q_{F6:n}^{i}}{K_{eff}} * m_i \right) - Q_{\gamma p} \qquad \text{Equation 3.2-8}$$

Such that:
Q_{fp} = energy released per fission (MeV/fission) due to fission products
Q_n = energy released per fission (MeV/fission) due to neutrons
$Q_{\gamma p}$ = energy released per fission (MeV/fission) due to prompt gammas
$Q_{\gamma c}$ = energy released per fission (MeV/fission) due to capture gammas
v = average number of neutrons per fission
m_i = mass of material in cell i
i = cells in MCNP model
K_{eff} = eigenvalue of the system

From the MCNP output files, the average number of neutrons per fission and the mass of material in each cell can be obtained. The K_{eff} of the system is assumed to be 1 unless otherwise specified. The resulting Q-values from the MCNP6 simulations are detailed in Section 4.

To calculate the power and volumetric heating rates in each cell the F4:n tally in the MCNP6 simulation is used with multiplier cards from reference [13]. By using the atom density, the fuel material, the microscopic fission cross section, and the fission energy, MCNP is able to convert the tally into a local power output of W/cm^3. The material must be selected as well as using the -6 and -8 option cards. These particular tallies are determined by multiplying the reactor thermal power, the number of fission neutrons per fission (2.442) and divining by the fissions per MeV (197.7). The multiplier tally for the three different reactors is provided in Table 3.2-1. Using the F4:n tally with a multiplier card using the atom density, material and the 1 and -4 options MCNP will produce a result for energy released due to neutron interactions in w/cm^3. To obtain the FM4 multiplier for the cell average neutron flux the multiplier becomes the reactor power multiplied by, the number of fission neutrons per fission (2.442) and divining by the fissions per MeV (197.7) divided by the number of MeV per Joule (1.602E-13).

Table 3.2-1: Test Sample Tally Information

Test Sample Tally Information			
Parameter	TRIGA	HFIR	ATR
Reactor Thermal Power (MW)	1.0	85.0	22.0
FM4 Multiplier (W/cm^3)	1.2352E4	1.04992E6	2.2717E5
FM4 Multiplier (n/(cm^2*s))	7.71355E16	6.55651E18	1.69698E18

*See references [11] and [13]

Using the convective heat transfer equations on Figure 3.2-1, the temperature of the capsule can be estimated at different internal positions.

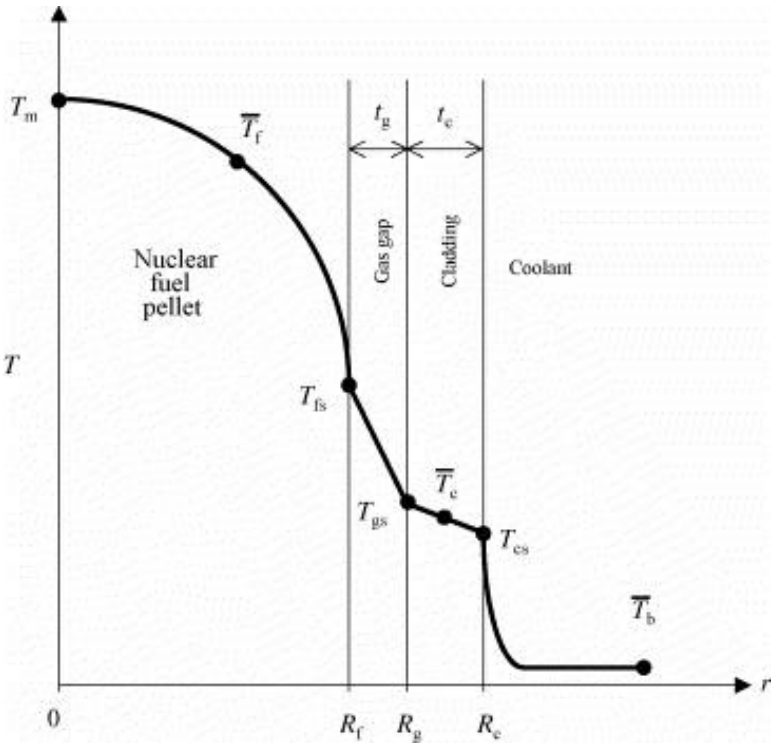

Figure 3.2-1 Capsule Heat Transfer Diagram.

To determine the outer surface temperature of the capsule Equation 3.2-9 is used from reference [25].

$$T_{co} - T_b = \frac{q'(z)}{2\pi h_b R_c} \qquad \text{Equation 3.2-9}$$

Where the variables are defined as:

R_c = The outer radius of the capsule (cm)
h_b = The convective heat transfer coefficient for the pool
T_b = The temperature of the pool (k)
T_{co} = External temperature of the capsule (K)
q'= Energy generation per distance (W/cm)

The temperature of the pool for each case is set to 310 K and the radius of each capsule can be found in the section 3.1. The energy generated per unit volume is determined from the MCNP results and converted to q'. To determine the convective heat transfer coefficient several different equations from refence [12], need to be applied to determine the Nusselt number.

$$h_b = \frac{Nu * k}{L} \qquad \text{Equation 3.2-10}$$

Such that:

L = Length of the capsule (cm)
K = The thermal conductivity of the water at 20 C (.6 W/m)
g = Gravity (9.8 m/s^2)

$$Pr = \frac{v}{\alpha} \qquad \text{Equation 3.2-11}$$

$$Gr_L = \frac{g\beta(T_{co} - T_b)L^3}{v^2} \qquad \text{Equation 3.2-12}$$

$$Ra_L = Gr_L * Pr \qquad \text{Equation 3.2-13}$$

For water at 310 K the following parameters can be used.

β = Volumetric expansion coefficient (.000303 1/C)
v = Kinematic Viscosity (.8007*10^-6 m^2/s)
Pr = Prandtl number 5.43

The equation used for vertical flow free convection from reference [12] equation 9.26 is being used for the TRIGA model is below.

$$Nu = \left(.825 + \frac{\left(.387 Ra_L^{\frac{1}{6}} \right)}{\left(1 + \left(\frac{.492}{\Pr} \right)^{\frac{9}{16}} \right)^{\frac{8}{27}}} \right)^2 \qquad \text{Equation 3.2-14}$$

Using the length of 4 inches for the capsule and an assume temperature differential of 100 K the Nu and thus h for the TRIGA capsule can be calculated. The resulting Nu is 203 and a value of $h = 1201$ w/m^2*k.

For the HFIR and ATR reactors the equations to determine Nu is from reference [12] used for flat plates with constant heat flux equation 7.46. For a long cylinder in a turbulent flow region this equation will work for determining Nu number.

$$Re = \frac{VL}{v} \qquad \text{Equation 3.2-15}$$

Such at:

V = Velocity of fluid m/s

$$Nu = .0308 Re_L^{\frac{4}{5}} \Pr^{\frac{1}{3}} \qquad \text{Equation 3.2-16}$$

To determine the velocity of HFIR first we start with the mass flow rate of .82 m^3/s with a 15 inches core diameter from reference [26]. This results in an average flow velocity through the core of 7.2 m/s before reaching the 18-inch diameter exit pipe. This results in a Nu number of 2.2249e+03 and a convective heat transfer coefficient of 2.0514*10^4 w/m^2*k.

According to refence [16] the flux traps at ATR have a maximum flow rate of 80 gpm (0.0050472 m^3/s) with the flux trap from [27] having a diameter of 7.62 cm. This results in a velocity of 1.11 m/s. This results in a Nu number of 1.4307*10^3 and a convective heat transfer coefficient of 3.5211*10^3 w/m^2*k.

To calculate the interior wall temperature of the capsule Equation 3.2-17 is used.

$$T_{ci} - T_{co} = \frac{q'(z)}{\frac{2\pi k_c}{\ln(R_c/R_g)}} \qquad \text{Equation 3.2-17}$$

Where the variables are defined as:

R_c = The outer radius of the capsule (cm)
R_g = The inner radius of the capsule (cm)
K_c = The thermal conductivity of the capsule
T_{ci} = Internal temperature of the capsule (K)
T_{co} = External temperature of the capsule (K)
q'= Energy generation per distance (W/cm)

The thermal conductivity used for the aluminum capsules is 205 w/m*k while the stainless steel zirc capsules has a thermal conductivity 16 w/m*k.

To determine the temperature of the fuel exterior across the air gap Equation 3.2-18 is used

$$T_{fs} - T_{ci} = \frac{q'(z)}{2\pi h_{gap} R_g} \qquad \text{Equation 3.2-18}$$

Such that:
R_g = The inner radius of the capsule (cm)
h_{gap} = The convective heat transfer coefficient for the gap
T_{ci} = Internal temperature of the capsule (K)
T_{fs} = Surface temperature of the fuel (K)
q'= Energy generation per distance (W/cm)

The gap convective heat transfer coefficient used for this experiment come from reference [28] page 422 and is 10 w/cm^2*k

For calculating the centerline temperature of the fuel sample Equation 3.2-19 is used.

$$T_m - T_{fs} = \frac{q'(z)}{4\pi K_f} \qquad \text{Equation 3.2-19}$$

Such that:
K_f = The thermal conductivity of the test sample
T_{fs} = Surface temperature of the fuel (K)
T_m = Centerline temperature of the fuel (K)
q'= Energy generation per distance (W/cm)

The thermal conductivity of the test sample comes from reference [29] and is set as .05 w/cm*k.

These equations and its assumptions should result in a conservative bias for the temperature of the capsule because it ignores heat transfer out of the top and bottom of the capsule and assumes that it is infinitely long. These conservatisms will ensure that the capsule has an appropriate margin.

4. Results

In this section, a presentation of the TRIGA, HFIR, and ATR MCNP results are provided for the hafnium carbide (HfC-ZrC), depleted uranium carbide (DUC-ZrC), and uranium carbide (UC-ZrC) test samples. The cell numbers correspond to the 10 equal size segments of the test sample starting from the bottom up. These numbers correspond directly to the MCNP volumes used in the simulation. The tally results in this section will be used in conjunction with equation 3.2-13 to determine a maximum capsule temperature as a result of the fuel and fuel surrogate exposure to the reactor. The three different tally results presented in the tables represent three different parameters. The tally with units (W/cm^3) represent the thermal power generated by the sample due to fission. The tally with units n/(cm^2 s) represent the call average neutron flux. Finally, the F_6 tally represent the amount of heat produced in MeV per gram fission caused by fission products and neutron interaction. The error presented in this section was obtained from the MCNP output files. This error is associated with the nature Monte Carlo method used to obtain the results, this is mentioned in section 3.

4.1. TRIGA Capsule

Table 4.1-1 summarizes the MCNP results for the surrogate fuel sample (HfC-ZrC) placed inside the TRIGA core model in the ICIT configuration. The sample did not generate a thermal output due to fission and this is as expected of the surrogate material. The flux tally results and the associated error are also presented in this table. The surrogate material performed as expected of a test sample without fissionable material and should not produce a limiting scenario for the capsule.

Table 4.1-1: TRIGA Core HfC-ZrC Results

TRIGA Core HfC-ZrC					
Cell Number Test sample	Volumetric Fission Power W/cm^3	Neutron Volumetric Heating W/cm^3	Neutron Volumetric Heating Fractional Error	Local Neutron Flux n/(cm^2*s)	Local Neutron Flux Fractional Error
cell 18544	0.00E+00	4.05E-06	0.0546	2.16E+13	2.96E-02
cell 18545	0.00E+00	4.08E-06	0.0568	2.16E+13	2.96E-02
cell 18546	0.00E+00	4.27E-06	0.0544	2.19E+13	2.92E-02
cell 18547	0.00E+00	3.88E-06	0.0537	2.42E+13	2.86E-02
cell 18548	0.00E+00	4.41E-06	0.0542	2.30E+13	2.88E-02
cell 18549	0.00E+00	3.96E-06	0.055	2.22E+13	2.94E-02
cell 18550	0.00E+00	4.24E-06	0.0571	2.35E+13	2.94E-02
cell 18551	0.00E+00	3.76E-06	0.0573	2.27E+13	2.90E-02
cell 18552	0.00E+00	3.95E-06	0.0568	2.23E+13	2.97E-02
cell 18553	0.00E+00	3.82E-06	0.0568	2.12E+13	3.00E-02

Table 4.1-2 summarizes the MCNP results for the test sample (DUC-ZrC) placed inside the TRIGA core model in the ICIT configuration. The sample did generate a thermal output due to fission. The sample produced a small amount of thermal power in the presence of a neutron rich environment, this is due to the depleted uranium in the test sample. The tally results and the associated error are also presented in Table 4.1-2. The surrogate material simulated inside a reactor has peak neutron flux near the center of the capsule. This results in an increased volumetric fission power in those areas with it slightly decreasing on either end. The results and tallies will be further evaluated in section 5.

Table 4.1-2: TRIGA Core DUC-ZrC Results

TRIGA Core DUC-ZrC				
Cell Number	Local Neutron Flux n/(cm^2*s)	Local Neutron Flux Fractional Error	MCNP heating rate MeV/g-fission neutron	MCNP heating rate Fractional Error
cell 18544	1.95E+13	0.0297	3.69E-06	0.0572
cell 18545	2.08E+13	0.0291	3.42E-06	0.0569
cell 18546	2.20E+13	0.028	3.90E-06	0.0564
cell 18547	2.07E+13	0.0283	3.60E-06	0.056
cell 18548	2.12E+13	0.0282	3.77E-06	0.0556
cell 18549	2.07E+13	0.0289	3.67E-06	0.0566
cell 18550	2.11E+13	0.029	3.95E-06	0.0561
cell 18551	2.06E+13	0.0296	3.52E-06	0.0558
cell 18552	2.12E+13	0.0289	3.74E-06	0.0571
cell 18553	2.05E+13	0.0292	3.66E-06	0.0594
Cell Number	Volumetric Fission Power W/cm^3	Volumetric Fission Power Fractional Error	Neutron Volumetric Heating W/cm^3	Neutron Volumetric Heating Fractional Error
cell 18544	1.29E-01	0.0588	1.36E-05	0.0572
cell 18545	1.16E-01	0.0594	1.26E-05	0.0569
cell 18546	1.36E-01	0.0584	1.44E-05	0.0564
cell 18547	1.25E-01	0.0585	1.33E-05	0.056
cell 18548	1.30E-01	0.0572	1.39E-05	0.0556
cell 18549	1.26E-01	0.0581	1.35E-05	0.0566
cell 18550	1.36E-01	0.058	1.46E-05	0.0561
cell 18551	1.19E-01	0.0587	1.30E-05	0.0558
cell 18552	1.29E-01	0.0595	1.38E-05	0.0571
cell 18553	1.26E-01	0.0606	1.35E-05	0.0594

Table 4.1-3 summarizes the MCNP results for the test sample (UC-ZrC) placed inside the TRIGA core model in the ICIT configuration. The sample did generate a thermal output due to fission as this material does include LEU fuel and should produce a

thermal power output. The sample produced a thermal power in the presence of a neutron rich environment and is significantly larger than the other two test samples. The tally results and the associated error are also presented in this table. The test results bellow shows a peak in neutron flux and energy released in the center of the capsule due to fission because of an increased number of neutrons near the middle of the reactor. This causes an increased number neutron interaction in the test sample. The test sample tally results will be evaluated in section 5.

Table 4.1-3: TRIGA Core UC-ZrC Results

TRIGA Core UC-ZrC				
Cell Number	Local Neutron Flux n/(cm^2*s)	Local Neutron Flux Fractional Error	MCNP heating rate MeV/g-fission neutron	MCNP heating rate Fractional Error
cell 18544	3.18E+13	0.0295	6.57E-05	0.0329
cell 18545	3.43E+13	0.0291	6.28E-05	0.0331
cell 18546	3.70E+13	0.0279	7.07E-05	0.0329
cell 18547	3.67E+13	0.028	6.86E-05	0.0318
cell 18548	3.70E+13	0.0277	6.84E-05	0.0305
cell 18549	3.63E+13	0.028	6.96E-05	0.0385
cell 18550	3.77E+13	0.0278	6.92E-05	0.035
cell 18551	3.70E+13	0.0286	7.23E-05	0.0349
cell 18552	3.44E+13	0.0289	7.03E-05	0.0351
cell 18553	3.31E+13	0.0292	6.63E-05	0.0326
Cell Number	Volumetric Fission Power W/cm^3	Volumetric Fission Power Fractional Error	Neutron Volumetric Heating W/cm^3	Neutron Volumetric Heating Fractional Error
cell 18544	3.11E+00	0.0335	2.42E-04	0.0329
cell 18545	2.96E+00	0.0338	2.32E-04	0.0331
cell 18546	3.35E+00	0.0336	2.61E-04	0.0329
cell 18547	3.24E+00	0.0325	2.53E-04	0.0318
cell 18548	3.24E+00	0.0311	2.52E-04	0.0305
cell 18549	3.30E+00	0.0394	2.57E-04	0.0385
cell 18550	3.28E+00	0.0358	2.55E-04	0.035
cell 18551	3.42E+00	0.0357	2.66E-04	0.0349
cell 18552	3.34E+00	0.0358	2.59E-04	0.0351
cell 18553	3.14E+00	0.0333	2.44E-04	0.0326

Table 4.1-4 summarizes the MCNP results for the surrogate fuel sample (HfC-ZrC) placed inside a sphere of water with the predicted TRIGA ICIT flux profile facing inward. The sample did not generate a thermal output due to fission and this is as expected of the surrogate material without fissionable material. The neutron flux tally

results and the associated error are also presented in this table. The results of the tallies will be evaluated in section 5 but should not result in a limiting scenario.

Table 4.1-4: TRIGA Capsule HfC-ZrC Results

TRIGA Capsule HfC-ZrC					
Cell Number	Volumetric Fission Power W/cm^3	Neutron Volumetric Heating W/cm^3	Neutron Volumetric Heating Fractional Error	Local Neutron Flux n/(cm^2*s)	Local Neutron Flux Fractional Error
cell 3	0.00E+00	3.60E-06	0.0307	2.05E+13	0.0166
cell 4	0.00E+00	4.21E-06	0.0286	2.27E+13	0.015
cell 5	0.00E+00	4.31E-06	0.0277	2.37E+13	0.0144
cell 6	0.00E+00	4.27E-06	0.028	2.40E+13	0.0144
cell 7	0.00E+00	4.60E-06	0.0271	2.45E+13	0.0143
cell 8	0.00E+00	4.42E-06	0.0272	2.45E+13	0.0141
cell 9	0.00E+00	4.22E-06	0.0275	2.40E+13	0.0143
cell 10	0.00E+00	4.38E-06	0.0281	2.37E+13	0.0145
cell 11	0.00E+00	4.23E-06	0.0284	2.27E+13	0.0151
cell 12	0.00E+00	3.46E-06	0.0316	1.98E+13	0.0168

Table 4.1-5 summarizes the MCNP results for the test sample (DUC-ZrC) inside a sphere of water with the predicted TRIGA ICIT flux profile facing inward. The sample did generate a thermal output due to fission. The sample produced a small amount of thermal power in the presence of a neutron rich environment. The neutron flux tally results and the associated error are also presented in this table. The local neutron flux at the center of test sample is increased due to the isotropic distribution of neutrons and decreased leakage at the center. This cause the neutron flux and volumetric fission power to peak at the center of the capsule instead of the ends. The tally results will be evaluated in more detail in section 5.

Table 4.1-5: TRIGA Capsule DUC--ZrC Results

TRIGA Capsule DUC-ZrC				
Cell Number	Local Neutron Flux n/(cm^2*s)	Local Neutron Flux Fractional Error	MCNP heating rate MeV/g-fission neutron	MCNP heating rate Fractional Error
cell 3	2.84E+13	0.0151	2.76E-05	0.0174
cell 4	3.17E+13	0.0137	2.95E-05	0.0157
cell 5	3.33E+13	0.0131	3.08E-05	0.015
cell 6	3.39E+13	0.0128	3.15E-05	0.0149
cell 7	3.45E+13	0.0127	3.19E-05	0.0148
cell 8	3.49E+13	0.0126	3.23E-05	0.0147
cell 9	3.43E+13	0.0128	3.19E-05	0.0148
cell 10	3.36E+13	0.013	3.12E-05	0.015
cell 11	3.17E+13	0.0138	2.95E-05	0.016
cell 12	2.74E+13	0.0154	2.65E-05	0.0177
Cell Number	Volumetric Fission Power W/cm^3	Volumetric Fission Power Fractional Error	Neutron Volumetric Heating W/cm^3	Neutron Volumetric Heating Fractional Error
cell 3	1.293E+00	0.0178	1.02E-04	0.0174
cell 4	1.380E+00	0.016	1.09E-04	0.0157
cell 5	1.441E+00	0.0153	1.14E-04	0.015
cell 6	1.473E+00	0.0152	1.16E-04	0.0149
cell 7	1.490E+00	0.0151	1.18E-04	0.0148
cell 8	1.510E+00	0.0151	1.19E-04	0.0147
cell 9	1.495E+00	0.0151	1.18E-04	0.0148
cell 10	1.456E+00	0.0153	1.15E-04	0.015
cell 11	1.376E+00	0.0163	1.09E-04	0.016
cell 12	1.243E+00	0.0181	9.78E-05	0.0177

Table 4.1-6 summarizes the MCNP results for the test sample (UC-ZrC) inside a sphere of water with the predicted TRIGA ICIT flux profile facing inward. The sample did generate a thermal output due to fission as this material does include LEU fuel and should produce a thermal power output. The sample produced a thermal power in the

presence of a neutron rich environment and is significantly larger than the other two test samples. The surrogate material released a larger amount of fission energy than the other two test sample as a result of the material enrichment. The neutron flux and volumetric fission power also increased near the center of the capsule as a result of the neutron distribution. This also resulted in a more limiting scenario than the full core model of the same test sample. The tally results will be evaluated in section 5.

Table 4.1-6: TRIGA Capsule UC-ZrC Results

TRIGA Capsule UC-ZrC				
Cell Number	Local Neutron Flux n/(cm^2*s)	Local Neutron Flux Fractional Error	MCNP heating rate MeV/g-fission neutron	MCNP heating rate Fractional Error
cell 3	2.85E+13	0.0154	1.09E-03	0.0205
cell 4	3.23E+13	0.0139	1.12E-03	0.0186
cell 5	3.38E+13	0.0132	1.16E-03	0.018
cell 6	3.40E+13	0.0129	1.15E-03	0.0176
cell 7	3.51E+13	0.0128	1.15E-03	0.0176
cell 8	3.52E+13	0.0128	1.17E-03	0.0175
cell 9	3.44E+13	0.013	1.15E-03	0.0178
cell 10	3.38E+13	0.0132	1.13E-03	0.0177
cell 11	3.23E+13	0.0138	1.10E-03	0.0188
cell 12	2.78E+13	0.0155	1.07E-03	0.0206
Cell Number	Volumetric Fission Power W/cm^3	Volumetric Fission Power Fractional Error	Neutron Volumetric Heating W/cm^3	Neutron Volumetric Heating Fractional Error
cell 3	5.30E+01	0.0206	4.02E-03	0.0205
cell 4	5.44E+01	0.0186	4.12E-03	0.0186
cell 5	5.62E+01	0.018	4.26E-03	0.018
cell 6	5.57E+01	0.0176	4.23E-03	0.0176
cell 7	5.60E+01	0.0176	4.24E-03	0.0176
cell 8	5.69E+01	0.0175	4.31E-03	0.0175
cell 9	5.61E+01	0.0178	4.25E-03	0.0178
cell 10	5.51E+01	0.0177	4.18E-03	0.0177
cell 11	5.37E+01	0.0188	4.07E-03	0.0188
cell 12	5.18E+01	0.0206	3.93E-03	0.0206

The TRIGA test results summarized above demonstrate two different simulation methods. The first method involves simulating the entire TRIGA reactor core and surrounding structure. The second method simulates an inward facing flux profile on a cylindrical surface surrounded by a water sphere. The results from the two test

scenarios produced similar values for measured neutron flux. However, the results from the cylindrical surface and surrounding water sphere test are more limiting than the full core model, this results in a more conservative simulation. Though the results for the flux of UC-ZrC are on average 7.96% smaller in the water sphere model the volumetric power is on average a 1,500% larger. For the DUC-ZrC material the neutron flux results are on average 55% larger in the water sphere model, the volumetric power is on average 1,000% larger.

Table 4.1-7 illustrated the cell by cell difference between the two modeling methods for volumetric power and neutron flux.

Table 4.1-7: Variance Water Sphere Model VS Full Core Model

Cell Number	HfC-ZrC % Difference Power	HfC-ZrC % Difference Flux	UC-ZrC % Difference Power	UC-ZrC % Difference Flux	DUC-ZrC % Difference Power	DUC-ZrC % Difference Flux
cell 3	-11.11	2.10	1,602.00	-10.35	904.14	46.01
cell 4	3.36	11.66	1,735.01	-5.98	1,092.94	52.14
cell 5	0.92	11.49	1,578.05	-8.61	961.66	51.70
cell 6	10.27	19.32	1,619.20	-7.22	1,078.82	63.37
cell 7	4.29	11.24	1,630.17	-5.07	1,043.65	62.81
cell 8	11.57	17.82	1,624.19	-3.26	1,096.19	68.34
cell 9	-0.40	16.42	1,612.05	-8.70	996.40	62.81
cell 10	16.51	17.57	1,509.85	-8.53	1,121.53	63.11
cell 11	7.16	8.86	1,510.06	-6.04	967.42	49.58
cell 12	-9.64	0.90	1,551.23	-15.84	887.14	33.35
Average	3.29	11.74	1,597.18	-7.96	1,014.99	55.32

4.2. HFIR Capsule

Table 4.2-1 summarizes the MCNP results for the surrogate fuel sample (HfC-ZrC) placed inside a sphere of water with the predicted HFIR position 4 flux profile facing inward. This section does not provide results for a full core HFIR MCNP simulation as a result of not having access to the MCNP model. The (HfC-ZrC) sample did not generate a thermal output due to fission and this is as expected of the surrogate material without fissionable material. The neutron flux tally results and the associated error are also presented in this table. This surrogate material should not produce a limiting scenario for the capsule.

Table 4.2-1: HFIR Capsule HfC-ZrC Results

HFIR Capsule HfC-ZrC					
Cell Number	Volumetric Fission Power W/cm^3	Neutron Volumetric Heating W/cm^3	Neutron Volumetric Heating Fractional Error	Local Neutron Flux n/(cm^2*s)	Local Neutron Flux Fractional Error
cell 3	0.00E+00	3.36E-05	0.0291	1.28E+15	4.25E-02
cell 4	0.00E+00	3.18E-05	0.0296	1.23E+15	4.41E-02
cell 5	0.00E+00	3.27E-05	0.0295	1.26E+15	4.15E-02
cell 6	0.00E+00	3.28E-05	0.0294	1.33E+15	4.18E-02
cell 7	0.00E+00	3.34E-05	0.0293	1.27E+15	4.16E-02
cell 8	0.00E+00	3.36E-05	0.0291	1.27E+15	4.20E-02
cell 9	0.00E+00	3.26E-05	0.0294	1.33E+15	4.03E-02
cell 10	0.00E+00	3.30E-05	0.0295	1.31E+15	4.16E-02
cell 11	0.00E+00	3.23E-05	0.0296	1.25E+15	4.24E-02
cell 12	0.00E+00	3.21E-05	0.0301	1.23E+15	4.23E-02

Table 4.2-2 summarizes the MCNP results for the test sample (DUC-ZrC) inside a sphere of water with the predicted HFIR position 4 flux profile facing inward. The sample did generate a thermal output due to fission as the test material includes depleted uranium. The sample produced a significant amount of thermal power in the presence of the HFIR simulated neutron rich environment. The tally results and the

associated error are also presented in this table. The neutron flux and volumetric fission power peak in the center similar to the full core TRIGA model and other models of this type. However, the flux results are larger due to the increased thermal power of the reactor and HFIR flux profile. The surrogate material and tallies will be evaluated in section 5.

Table 4.2-2: HFIR Capsule DUC-ZrC Results

HFIR Capsule DUC-ZrC				
Cell Number	Local Neutron Flux n/(cm^2*s)	Local Neutron Flux Fractional Error	MCNP heating rate MeV/g-fission neutron	MCNP heating rate Fractional Error
cell 3	1.37E+15	4.14E-02	1.62E-05	4.64E-02
cell 4	1.38E+15	4.30E-02	1.69E-05	5.15E-02
cell 5	1.40E+15	3.95E-02	1.71E-05	4.45E-02
cell 6	1.45E+15	4.00E-02	1.81E-05	4.54E-02
cell 7	1.39E+15	4.00E-02	1.69E-05	4.48E-02
cell 8	1.41E+15	4.02E-02	1.76E-05	4.56E-02
cell 9	1.47E+15	3.94E-02	1.76E-05	4.39E-02
cell 10	1.45E+15	3.99E-02	1.68E-05	4.37E-02
cell 11	1.41E+15	4.15E-02	1.74E-05	4.63E-02
cell 12	1.36E+15	4.06E-02	1.67E-05	4.46E-02
Cell Number	Volumetric Fission Power W/cm^3	Volumetric Fission Power Fractional Error	Neutron Volumetric Heating W/cm^3	Neutron Volumetric Heating Fractional Error
cell 3	6.14E+01	4.74E-02	3.69E-04	0.0197
cell 4	6.50E+01	5.31E-02	3.67E-04	0.0193
cell 5	6.51E+01	4.54E-02	3.64E-04	0.0189
cell 6	6.82E+01	4.65E-02	3.66E-04	0.0187
cell 7	6.42E+01	4.58E-02	3.69E-04	0.019
cell 8	6.69E+01	4.67E-02	3.72E-04	0.0188
cell 9	6.60E+01	4.49E-02	3.63E-04	0.0189
cell 10	6.35E+01	4.45E-02	3.72E-04	0.019
cell 11	6.52E+01	4.73E-02	3.70E-04	0.0194
cell 12	6.30E+01	4.55E-02	3.55E-04	0.0196

Table 4.2-3 summarizes the MCNP results for the test sample (UC-ZrC) inside a sphere of water with the predicted HFIR position 4 flux profile facing inward. The sample did generate a thermal output due to fission as this material does include LEU fuel and should produce a thermal power output. The sample produced a thermal power in the presence of a neutron rich environment and is significantly larger than the other two test samples due to the LEU in the sample. The volumetric fission power peaks in this test sample at 2900 w/cm^3 and is the largest of all 12 test cases. This is due to the test sample and HFIR flux profile. Like the other test cases the neutron flux and volumetric fission power peaks in the center of the test sample due to the simulated neutron distribution. The tally results and the associated error are presented in Table 4.2-3. The test sample and tally results will be evaluated in section 5.

Table 4.2-3: HFIR Capsule UC-ZrC Results

HFIR Capsule UC-ZrC				
Cell Number	Local Neutron Flux n/(cm^2*s)	Local Neutron Flux Fractional Error	MCNP Heating Rate MeV/g-fission neutron	MCNP Heating Rate Fractional Error
cell 3	1.38E+15	4.13E-02	6.37E-04	5.83E-02
cell 4	1.36E+15	4.34E-02	6.62E-04	6.08E-02
cell 5	1.42E+15	4.04E-02	6.52E-04	5.67E-02
cell 6	1.48E+15	4.05E-02	6.72E-04	5.91E-02
cell 7	1.40E+15	4.04E-02	6.52E-04	5.67E-02
cell 8	1.43E+15	4.08E-02	7.03E-04	5.99E-02
cell 9	1.51E+15	3.93E-02	6.79E-04	5.71E-02
cell 10	1.46E+15	4.02E-02	6.35E-04	5.63E-02
cell 11	1.40E+15	4.19E-02	6.30E-04	6.03E-02
cell 12	1.34E+15	4.14E-02	6.13E-04	5.78E-02
Cell Number	Volumetric Fission Power W/cm^3	Volumetric Fission Power Fractional Error	Neutron Volumetric Heating W/cm^3	Neutron Volumetric Heating Fractional Error
cell 3	2.63E+03	5.84E-02	1.35E-02	0.0258
cell 4	2.73E+03	6.09E-02	1.32E-02	0.0254
cell 5	2.69E+03	5.69E-02	1.31E-02	0.0246
cell 6	2.77E+03	5.93E-02	1.37E-02	0.0247
cell 7	2.69E+03	5.69E-02	1.35E-02	0.0247
cell 8	2.90E+03	6.00E-02	1.37E-02	0.0247
cell 9	2.80E+03	5.73E-02	1.35E-02	0.0248
cell 10	2.62E+03	5.64E-02	1.34E-02	0.0249
cell 11	2.60E+03	6.05E-02	1.37E-02	0.0247
cell 12	2.53E+03	5.80E-02	1.35E-02	0.0255

The HFIR results produce the most limiting scenario of any of the test cases. This is due to the increased neutron flux experience by the capsule. The flux results for the HFIR tests are more uniform across the capsules compared to the TRIGA test.

However, there is still some peaking in the center of the capsule due to the shape of the neutron flux source.

4.3. ATR Capsule

Table 4.3-1 summarizes the MCNP results for the surrogate fuel sample (HfC-ZrC) placed inside a sphere of water with the predicted ATR flux profile facing inward. This section does not provide results for a full core ATR MCNP simulation as a result of not having access to the ATR MCNP model. The HfC-ZrC sample did not generate a thermal output due to fission and this is as expected of the surrogate material without any fissionable material. The flux tally results and the associated error are also presented in this table. This surrogate material should not produce a limiting scenario for the capsule.

Table 4.3-1: ATR Capsule HfC-ZrC Results

ATR Capsule HfC-ZrC					
Cell Number	Volumetric Fission Power W/cm^3	Neutron Volumetric Heating W/cm^3	Neutron Volumetric Heating Fractional Error	Local Neutron Flux n/(cm^2*s)	Local Neutron Flux Fractional Error
cell 3	0.00E+00	2.17E-05	0.0187	1.95E+14	3.29E-02
cell 4	0.00E+00	2.22E-05	0.0182	2.28E+14	3.10E-02
cell 5	0.00E+00	2.25E-05	0.0179	2.26E+14	3.12E-02
cell 6	0.00E+00	2.28E-05	0.0179	2.38E+14	3.05E-02
cell 7	0.00E+00	2.30E-05	0.018	2.48E+14	2.94E-02
cell 8	0.00E+00	2.28E-05	0.0178	2.27E+14	3.01E-02
cell 9	0.00E+00	2.26E-05	0.018	2.34E+14	3.07E-02
cell 10	0.00E+00	2.25E-05	0.0181	2.34E+14	3.02E-02
cell 11	0.00E+00	2.26E-05	0.0181	2.18E+14	3.17E-02
cell 12	0.00E+00	2.04E-05	0.0191	1.83E+14	3.47E-02

Table 4.3-2 summarizes the MCNP results for the test sample (DUC-ZrC) inside a sphere of water with the predicted ATR flux profile on a 6-cm radius cylinder facing inward. The sample did generate a thermal output due to fission as expected of the test

material with depleted uranium. The sample produced a small amount of thermal power in the presence of a neutron rich environment. The neutron flux tally results and the associated error are also presented in this table. Volumetric fission power in this material peaks in the center of the sample as does the neutron flux. The results of the ATR simulation are much larger than the TRIGA results for the same sample but smaller than the HFIR results. The ATR DUC-ZrC results should be nonlimiting for this capsule design. The surrogate material will be evaluated in more detail section 5.

Table 4.3-2: ATR Capsule DUC-ZrC Results

ATR Capsule DUC-ZrC				
Cell Number	Local Neutron Flux n/(cm^2*s)	Local Neutron Flux Fractional Error	MCNP heating rate MeV/g-fission neutron	MCNP heating rate Fractional Error
cell 3	2.14E+14	3.27E-02	8.96E-06	3.74E-02
cell 4	2.52E+14	3.07E-02	1.04E-05	3.55E-02
cell 5	2.52E+14	3.05E-02	1.10E-05	3.59E-02
cell 6	2.76E+14	2.97E-02	1.19E-05	3.39E-02
cell 7	2.84E+14	2.84E-02	1.22E-05	3.26E-02
cell 8	2.70E+14	3.00E-02	1.19E-05	3.36E-02
cell 9	2.61E+14	2.95E-02	1.14E-05	3.37E-02
cell 10	2.66E+14	2.98E-02	1.14E-05	3.32E-02
cell 11	2.41E+14	3.10E-02	1.05E-05	3.51E-02
cell 12	2.03E+14	3.38E-02	8.82E-06	3.85E-02
Cell Number	Volumetric Fission Power W/cm^3	Volumetric Fission Power Fractional Error	Neutron Volumetric Heating W/cm^3	Neutron Volumetric Heating Fractional Error
cell 3	7.12E+00	3.94E-02	2.03E-04	0.0153
cell 4	8.37E+00	3.73E-02	2.32E-04	0.0145
cell 5	8.97E+00	3.76E-02	2.41E-04	0.0141
cell 6	9.72E+00	3.55E-02	2.38E-04	0.0139
cell 7	9.90E+00	3.40E-02	2.39E-04	0.014
cell 8	9.71E+00	3.51E-02	2.48E-04	0.014
cell 9	9.31E+00	3.51E-02	2.41E-04	0.0141
cell 10	9.30E+00	3.45E-02	2.37E-04	0.0141
cell 11	8.48E+00	3.67E-02	2.24E-04	0.0145
cell 12	7.12E+00	4.03E-02	1.89E-04	0.0155

Table 4.3-3 summarizes the MCNP results for the test sample (UC-ZrC) inside a sphere of water with the predicted ATR flux profile facing inward. The sample did generate a thermal output due to fission as this material does include LEU fuel and should produce a thermal power output. The sample produced a thermal power in the presence of a

neutron rich environment and is significantly larger than the other two test samples because of the LEU in the test sample. The local neutron flux of the ATR sample also peaks in the center due to the shape of the source distribution. This result in a higher volumetric fission power near the center of the capsule due to the increased neutron flux. The tally results and the associated error are also presented in Table 4.3-3. The test sample will be evaluated further in section 5.

Table 4.3-3: ATR Capsule UC-ZrC Results

ATR Capsule UC-ZrC				
Cell Number	Local Neutron Flux n/(cm^2*s)	Local Neutron Flux Fractional Error	MCNP heating rate MeV/g-fission neutron	MCNP heating rate Fractional Error
cell 3	2.11E+14	3.24E-02	2.68E-04	5.27E-02
cell 4	2.55E+14	3.06E-02	3.59E-04	4.97E-02
cell 5	2.55E+14	3.02E-02	3.88E-04	4.86E-02
cell 6	2.68E+14	2.94E-02	4.05E-04	4.52E-02
cell 7	2.88E+14	2.88E-02	4.20E-04	4.50E-02
cell 8	2.69E+14	2.97E-02	3.90E-04	4.51E-02
cell 9	2.68E+14	3.01E-02	4.01E-04	4.67E-02
cell 10	2.73E+14	3.00E-02	4.07E-04	4.54E-02
cell 11	2.48E+14	3.12E-02	3.61E-04	5.14E-02
cell 12	2.04E+14	3.39E-02	2.77E-04	5.39E-02
Cell Number	Volumetric Fission Power W/cm^3	Volumetric Fission Power Fractional Error	Neutron Volumetric Heating W/cm^3	Neutron Volumetric Heating Fractional Error
cell 3	2.39E+02	5.29E-02	6.40E-03	0.0222
cell 4	3.20E+02	4.99E-02	7.80E-03	0.02
cell 5	3.46E+02	4.87E-02	8.10E-03	0.0197
cell 6	3.61E+02	4.53E-02	8.19E-03	0.0194
cell 7	3.75E+02	4.51E-02	8.24E-03	0.0194
cell 8	3.49E+02	4.52E-02	8.29E-03	0.0193
cell 9	3.58E+02	4.69E-02	8.12E-03	0.0197
cell 10	3.64E+02	4.55E-02	8.05E-03	0.0199
cell 11	3.22E+02	5.16E-02	7.40E-03	0.0207
cell 12	2.47E+02	5.40E-02	6.20E-03	0.023

The results for the ATR profile are similar in shape to the full core model, this is because of the cylindrical flux profile used for modeling these test cases. The power and flux tally results for the ATR reactor are more limiting than the TRIGA models but are less limiting than the HFIR model. This is to be expected based off the flux profile

and simulated thermal power of the ATR reactor. These results may not result in the most limiting scenario for any of the capsule designs but will still be evaluated in section 5 to see the effect on the capsule.

5. Discussion

Section 4 presents the MCNP results for the three different capsule designs for the three different reactor types. This section will discuss the MCNP results from section 4 and the importance behind them. The four different tallies in section 4 represent different simulated results experienced by the capsule. By using the tables from section 4 and Equation 3.2-6, the energy released by neutrons and fission products per fission can be determined. This is represented by the fifth column in Table *5-1* as $Q_{fp}\ and\ Q_n$. The HFIR results are the most limiting for the $Q_{fp}\ and\ Q_n$ parameters with a maximum value of 4.82E-01MeV/fission for the (UC-ZrC) test sample. This is most likely due to the size of the HFIR sample and the flux spectrum. These results can be used to determine the additional heating caused by the fission products and fission neutrons.

By using Equation 3.2-17 through Equation 3.2-19, the described parameters of each capsule in section 3.1, and the volumetric fission power tallies (W/cm^3) and neutron heating tallies (w/cm^3) from section 4, a conservative estimate of the maximum capsule internal temperatures can be made. In addition, by applying these equations to the internal edge of the capsule the capsule internal temperature can also be estimated. The assumed surrounding pool temperature is 310 K. For the 12 test cases the results of these calculation are included in Table 5-1.

Table 5-1: Capsule Temperatures

Test Sample Type	Center Line Fuel Temperature (K)	Outer surface of Fuel Temperature (K)	Internal capsule Temperature (K)	Outer Surface capsule Temperature (K)	Q_{fp} and Q_n (MeV/fission)
TRIGA Core HfC-ZrC	310.00	310.00	310.00	310.00	0.00E+00
TRIGA Core DUC-ZrC	310.96	310.41	310.41	310.40	8.04E-04
TRIGA Core UC-ZrC	334.20	320.33	320.19	320.10	1.49E-02
TRIGA Capsule HfC-ZrC	310.00	310.00	310.00	310.00	0.00E+00
TRIGA Capsule DUC-ZrC	320.67	314.56	314.49	314.46	6.59E-03
TRIGA Capsule UC-ZrC	694.24	474.04	471.84	470.41	2.46E-01
HFIR Capsule HfC-ZrC	310.00	310.00	310.00	310.00	0.00E+00
HFIR Capsule DUC-ZrC	342.84	314.16	313.27	312.52	1.61E-02
HFIR Capsule UC-ZrC	1,706.27	486.82	449.16	417.13	4.82E-01

Test Sample Type	Center Line Fuel Temperature (K)	Outer surface of Fuel Temperature (K)	Internal capsule Temperature (K)	Outer Surface capsule Temperature (K)	Q_{fp} and Q_n (MeV/fission)
ATR Capsule HfC-ZrC	310.00	310.00	310.00	310.00	0.00E+00
ATR Capsule DUC-ZrC	337.02	321.26	320.89	317.61	2.36E-03
ATR Capsule UC-ZrC	864.45	541.07	533.41	466.19	8.00E-02

The increases in temperature in Table 5-1 are only accounting for the energy released due to fission and neutron interaction. The volumetric fission power and volumetric neutron heating are added together to determine a total volumetric power. This is multiplied by pi and the squared radius of test sample to obtain the heat transfer rate to generate Table 5-1 and is included in Table 5-2. These values are the maximum volumetric power results from the MCNP simulations. The error for these values has a range of 3-7%. However, the volumetric power results can vary by orders of magnitude because of fuel type or reactor type, thus the 3-7% error associated with the results are negligible. The increase in reactor temperature by the capture of excess fission neutrons and the subsequent gamma and beta decay of activation products is not accounted for in Table 5-1. However, these are typically considered a small portion of the total energy released and could be lost by the 3-7% statistical error.

Table 5-2: Capsule Volumetric Fission Power Value Results

Capsule Type	Maximum Volumetric Power (w/cm^3)	Heat Transfer Rate (w/cm)
TRIGA Core HfC-ZrC	4.41E-06	1.12E-05
TRIGA Core DUC-ZrC	1.36E-01	3.47E-01
TRIGA Core UC-ZrC	3.42E+00	8.71E+00
TRIGA Capsule HfC-ZrC	4.60E-06	1.17E-05
TRIGA Capsule DUC-ZrC	1.510E+00	3.843E+00
TRIGA Capsule UC-ZrC	5.44E+01	1.38E+02
HFIR Capsule HfC-ZrC	3.36E-05	8.87E-06
HFIR Capsule DUC-ZrC	6.82E+01	1.80E+01
HFIR Capsule UC-ZrC	2.90E+03	7.66E+02
ATR Capsule HfC-ZrC	2.30E-05	1.24E-05
ATR Capsule DUC-ZrC	5.46E+01	9.90E+00
ATR Capsule UC-ZrC	3.75E+02	2.03E+02

The thermal results inTable 5-1 are based on the assumed pool temperature of 310 K and a constant thermal conductivity in each section of the capsule specified in section 3.2. With these assumptions, the worst-case scenario for fuel center line temperature resulted from the HFIR reactor core flux and capsule model with the 19.9% enriched UC-ZrC test sample. The predicted internal test sample temperature is 1,700 Kelvin while the capsules internal wall temperature is predicted to be 450 Kelvin. The worst-case scenario for internal capsule temperature is the ATR capsule model with the 19.9% enriched UC-ZrC test sample with a center line temperature of 864 Kelvin and a interior

capsule wall temperature of 533 Kelvin. Aluminum with a melting point of 933.5 Kelvin the structural integrity of the aluminum capsule will be preserved. After a cooling period the test samples (DU and U) should produce significantly less thermal energy due to fission reactions and the overall capsule temperature show be reduced.
It is a conservative estimate that an additional 5% thermal power relative to the maximum thermal energy released for each core model should be added to each test case as a result of decay products inside the sample. With the inclusion of a 5% increase in thermal power the structural integrity of the aluminum capsule should still be maintained. Based on the results from Table 5-1, the thermal power released due to fission should not result in the degradation of the capsule or the test material.

Another concern is the criticality of the reactor core with the addition of the test samples. Table 5-3 shows the MCNP estimated K effective and standard deviation for the 3 different full core simulations. Two of the samples, the HfC-ZrC and the DUC-ZrC, should act as a thermal neutron poison, which would reduce the simulated k-effective value while the UC-ZrC should increase the value.

Table 5-3: TRIGA MCNP K Value

Test Sample:	TRIGA Core HfC-ZrC	TRIGA Core DUC-ZrC	TRIGA Core UC-ZrC
K value	0.99748, STD 0.00046	0.99730, STD 0.00046	0.99792, STD 0.00044

Based on the results from Table 5-3 it is apparent that the k-effective value was indeed affected by the sample in the capsule. However, the effect on the k-effective value as a result of the samples is in the range of .0005. This should be a considered effect before placing the sample into an active core. However, this is within one standard deviation of the calculated K-effective results from MCNP and could be a result of statistical error. Additional simulations in MCNP could be run to reduce the statistical error to identify the effect of the fuel sample on the reactor core more clearly. However, the effect of the test samples on the simulated K-effective of the reactor core is small enough so that it should not cause a major concern.

Before irradiating the sample, it is important to consider how the sample will respond to the presence of neutrons, and if it will become radioactive and unsafe to handle. This is essential for the safety of the facility, the workers, and the public. Two of the samples DUC-ZrC and UC-ZrC are both fissionable materials and will produce fission products. It is essential to properly handle these materials after irradiation. In order to remove these samples from a reactor core after irradiation, additional shielding of the material will be required. It would be appropriate to treat these samples after irradiation as if they were spent fuel and shield them as such.

6. Conclusion

In conclusion, this study has modeled an initial characterization of the possible irradiation capsules for three different simulated surrogate space reactor fuels, HfC-ZrC, DUC-ZrC, and UC-ZrC and in three different test reactors, namely the OSU TRIGA, HFIR, and ATR. It has provided insight on the capsule design, the fuel interactions when in the presents of neutrons, as well as simulation of an irritated capsule and develop a design for irradiating fuel. Also by changing the material sample in the MCNP simulation it allows for newly developed fuel to be tested. Furthermore, a comparison of the test samples response on the reactor core and the thermal energy released due to fission is also included.

6.1. Limitations

This study employs a few assumptions to enable the analysis to procced, and therefore is limited in its accuracy by several factors. Most of the assumptions are addressed in the method section as part of calculating the capsule temperatures as a result of thermal power and the addition of heating from radiation interactions. This includes, modeling the heat transfer in 1D, assuming the pool is essentially infinite in size compared to the heat generated by the capsule. Additionally, based on the results from the two contrasting TRIGA capsule simulations in section 4.1 and the similarity of the results of the two models, it is assumed that a simulated reactor flux modeled around the capsule can be used as a replacement for modeling the entire core model. However, the study is furthered limited by not including the entire core models for the ATR and HFIR reactors. The simulation is also limited as a Monte Carlo simulation and does include intrinsic statistical error.

6.2. Future Work

There are areas of improvement and potential future work that should be considered for this analysis. The MCNP model for the ATR and HFIR reactors could provide a more accurate simulation of the neutron exposure the capsules would experience. This should provide a more accurate simulation than the measured flux profiles being simulated around the capsule model. It will also be required by both ATR and HFIR as part of the safety and criticality and control rod worth calculations that will be part of the safety analysis for those reactors with the capsules included.

Another area that could be improved on or enhanced is the heat transfer and calculated temperature of the capsule. In the future a dedicated heat transfer code such as RELAP would be the most accurate method to predict the capsules thermal properties and how the thermal power and neutron flux would affect the capsule system. In this calculation the 1-D heat diffusion equation and the resulting material and heat transfer assumption should result in high bias for resulting capsule temperature.

Finally, computer simulations are a good method for predicting what will happen but testing the capsules with the surrogate fuel sample inside a reactor environment is an important step in confirming the simulated values. One example is the use of the ATR-C reactor/critical facility at ATR to test the criticality and control worth effects of the capsules when placed in the ATR. This would be an important step before testing the depleted uranium or low enriched uranium samples in any of the simulated core models.

7. References

1) “Steps in the Development of Nuclear Thermal Propulsion Fuels,” Qualls, A. L. and Werner, James, 2017 IEEE Aerospace Conference, Big Sky, MT, March 2017.
2) “Technical Program Plan for the Advanced Gas Reactor Fuel Development and Qualification Program,” ORNL/TM/202-262, Oak Ridge National Laboratory, Oak Ridge, TN, April 2003.
3) “Nuclear Furnace-1 Test Report,” LA-5189-MS Informal Report, Los Alamos Scientific Laboratory, Los Alamos, NM, March 1973.
4) “Small Nuclear Rocket Engine and Stage Benchmark Model”, Schnitzler, Bruce G. and Borowski, Stanley K., Aiaa-2008-4949, July 2008.
5) “Radiation Center.” In-Core Irradiation Tube (ICIT) | Radiation Center | Oregon State University, radiationcenter.oregonstate.edu/core-irradiation-tube-icit
6) “Neutron Science at ORNL.” In-Vessel Irradiation Experiment Facilities at HFIR | Neutron Science at ORNL, neutrons.ornl.gov/hfir/in-vessel-irradiation.
7) Marshall, Frances M. “The Advanced Test Reactor National Scientific User Facility Overview.” www.iaea.org. 2013, www.iaea.org/OurWork/ST/NE/NEFW/Technical-Areas/RRS/documents/TM_Innovation/Gougar_ATR.pdf
8) Sunny, Eva E., et al. “HIGH-FIDELITY HEAT DEPOSITION ANALYSIS FOR THE HIGH FLUX ISOTOPE REACTOR.” Oak Ridge National Laboratory, 2017.
9) Betzler, Benjamin R., et al. “COUPLED NUCLEAR-THERMAL-HYDRAULIC CALCULATIONS FOR FORT ST. VRAIN REACTOR.” The 14th International Topical Meeting on Nuclear Reactor Thermal hydraulics, 25 Sept. 2011
10) Goorley, John T., 2013, MCNP6 User's Manual Rev 0, LA-CP-13-00634, Los Alamos National Laboratory, Los Alamos, NM.
11) “Approaches: MCNP Tallies.” Oregon State University. 2015, Corvallis, Oregon
12) Bergman, Theodore L. Fundamentals of heat and mass transfer. John Wiley & Sons, 2011

13) "Approaches: MCNP Tallies Updated." Oregon State University. 2017, Corvallis, Oregon
14) Morison, W. "Nuclear Power Generation." ILO Encyclopaedia of Occupational Health and Safety, Mar. 2011, www.iloencyclopaedia.org/part-xi/power-generation-and-distribution/item/615-nuclear-power-generation#POW_fig1
15) High Flux Isotope Reactor User Guide. Oak Ridge National Laboratory, Nov. 2015, neutrons.ornl.gov/sites/default/files/High%20Flux%20Isotope%20Reactor%20User%20Guide%202.0.pdf.
16) Ryskamp, John M., et al. Mixed Oxide Fuels Testing in the Advanced Test Reactor to Support Plutonium Disposition. Idaho National Engineering Laboratory, Nov. 1995, www.iaea.org/inis/collection/NCLCollectionStore/_Public/27/032/27032084.pdf.
17) McDuffee, J., et al. "DESIGN OF THE JP30 AND JP31 EXPERIMENTS." DOE/ER-0313/49, vol. 49, Dec. 2010.
18) Howard, Richard, et al. "Neutron Irradiation of Hydrided Cladding Material in HFIR—Summary of Initial Activities." Oak Ridge National Laboratory, 30 Mar. 2012.
19) Haslett, R. A. "SPACE NUCLEAR THERMAL PROPULSION PROGRAM FINAL REPORT." PL-TR-95-1064, May 1995.
20) Tajmar, Martin. Advanced space propulsion systems. Springer, 2003.
21) Schickler, R.A., et al. "Comparison of HEU and LEU neutron spectra in irradiation facilities at the Oregon State TRIGA® Reactor." Nuclear Engineering and Design, vol. 262, 2013, doi:10.1016/j.nucengdes.2013.05.004.
22) Appel, Brad. "Multi Physics Design and Simulation of a Tungsten-Cermet Nuclear Thermal Rocket." Texas A&M University, 1 Aug. 2012. Web. 2 Feb. 2015. http://repository.tamu.edu/bitstream/handle/1969.1/ETD-TAMU-2012-08-11649/APPEL-THESIS.pdf?sequence=2&isAllowed=y.
23) "Nuclear Reactors and Radioisotopes for Space." Nuclear Reactors for Space - World Nuclear Association, www.world-nuclear.org/information-library/non-power-nuclear-applications/transport/nuclear-reactors-for-space.aspx.

24) FINSETH, J. L. “OVERVIEW OF ROVER ENGINE TESTS FINAL REPORT.” NASA, Feb. 1991, ntrs.nasa.gov/archive/nasa/casi.ntrs.nasa.gov/19920005899.pdf.
25) Klein, Andrew. “Thermal Hydraulics Lecture 4.” OSU lecture, Corvallis, Oregon
26) https://neutrons.ornl.gov/hfir/core-assembly
27) Marshall, Frances. “The Advanced Test Reactor Capabilities and Experiments.” Science.energy.gov, 6 Aug. 2008, science.energy.gov/~/media/np/pdf/research/idpra/The%20Advanced%20Test%20Reactor%20Capabilities%20and%20Experiments.pdf.
28) Todreas, Neil E., and Mujid S. Kazimi. Nuclear systems. Taylor & Francis, 2011.
29) “Thermal Conductivity of Uranium Dioxide.” Iaea.org, 1966, www.iaea.org/inis/collection/NCLCollectionStore/_Public/34/065/34065217.pdf.

8. Appendices

8.1. Test Materials MCNP Code

```
C Graphite Fuel HfC-ZrC mix with 0.640 g/cc of HfC
C temp at 293 K
m2  40090.80c 0.0099844321
    40091.80c 0.0021773630
    40092.80c 0.0033281440
    40094.80c 0.0033727780
    40096.80c 0.0005433705
    6000.80c  0.1087380524
    72174.80c 4.1107-06
    72176.80c 1.3514-04
    72177.80c 4.7787-04
    72178.80c 7.0087-04
    72179.80c 3.4992-04
    72180.80c 9.0127-04
mt2 grph.18t


C Graphite Fuel UC-ZrC mix with .3% U235 with 0.640 g/cc of UC
C Temp at 293 K
m2  40090.80c 0.0099844321
    40091.80c 0.0021773630
    40092.80c 0.0033281440
    40094.80c 0.0033727780
    40096.80c 0.0005433705
    6000.80c  0.1087380524
    92235.80c 0.0000077075
    92238.80c 0.0025614663
mt2 grph.18t

C Graphite Fuel UC-ZrC mix with 19.9% U235 with 0.640 g/cc of UC
C temp at 300 K
m2  40090.80c 0.0099844321
    40091.80c 0.0021773630
    40092.80c 0.0033281440
    40094.80c 0.0033727780
    40096.80c 0.0005433705
    6000.80c  0.1087380524
    92235.80c 0.0005074118
    92238.80c 0.0020617620
mt2 grph.18t
```

8.2. Example MCNP Code

```
Triga Capsule Design
C Cell Cards
C  Material  Density (g/cm^3)  Surfaces
1    1      -2.7              -1 2        imp:n=1              $ aluminum container
2    4      -1.029e-3          -2 3        imp:n=1              $ air gap
3    2      -3.686            -3 -11      imp:n=1  vol=2.461733   $ fuels sample 1
4    2      -3.686            -3 -12 11    imp:n=1  vol=2.461733   $ fuels sample 2
5    2      -3.686            -3 -13 12    imp:n=1  vol=2.461733   $ fuels sample 3
6    2      -3.686            -3 -14 13    imp:n=1  vol=2.461733   $ fuels sample 4
7    2      -3.686            -3 -15 14    imp:n=1  vol=2.461733   $ fuels sample 5
8    2      -3.686            -3 -16 15    imp:n=1  vol=2.461733   $ fuels sample 6
9    2      -3.686            -3 -17 16    imp:n=1  vol=2.461733   $ fuels sample 7
10   2       -3.686            -3 -18 17    imp:n=1  vol=2.461733   $ fuels sample 8
11   2       -3.686            -3 -19 18    imp:n=1  vol=2.461733   $ fuels sample 9
12   2       -3.686            -3     19    imp:n=1  vol=2.461733   $ fuels sample 10
13   3        0.98465           -4 1        imp:n=1              $ water around container
14   0                         4          imp:n=0              $ void

C Surface Cards
C Units are in cm
C surface cards: the dimensions and locations of these cylinders need to be modified
C Capsule dimensions, 10.16 cm height, radius of 1.143 cm with a thickness of .143
cm
1 RCC 0 0 -5.08     0 0 10.16   1.143            $ outer surface of the Capsule
2 RCC 0 0 -4.937    0 0 9.874   1.00             $ Inner surface of the Capsule
3 RCC 0 0 -4.837    0 0 9.674   .900             $ air gap from capsule to fuel
c Added surfaces to divide Capsule into 10, .9674 cm axial segments
11  pz  -3.8696
12  pz  -2.9022
13  pz  -1.9348
14  pz  -0.9674
15  pz   0.0
16  pz   0.9674
17  pz   1.9348
18  pz   2.9022
19  pz   3.8696
4   SO   8.0          $ area around capsule water
5   CZ   4.3          $ cylinder on the Z axis with raidus 2.0 cm

C Create source a surface source around the target at 0 0 0
mode N
SDEF  SUR=5 dir=-1 POS=0 0 -5 RAD=4.3 EXT=d1 AXS=0 0 1 ERG=D2 $ The
Source is on the outer edge of surface 5 facing in ward
SI1 0 10
SP1 0 1
```

```
C Triga ICIT flux spectrum
#  SI2 SP2  $ the reactor source distribution
    0        0
    1.00E-10   4.50+09
    1.00E-09   4.53+11
    1.00E-08   1.35+12
    2.30E-08   2.89+12
    5.00E-08   1.81+12
    7.60E-08   1.43+12
    3.50E-06   4.11+11
    2.10E-05   3.74+11
    3.00E-05   4.95+11
    4.50E-05   5.92+11
    6.90E-05   5.81+11
    1.00E-04   5.14+11
    1.35E-04   4.33+11
    1.70E-04   5.26+11
    2.20E-04   5.19+11
    2.80E-04   5.60+11
    3.60E-04   5.19+11
    4.50E-04   5.77+11
    5.75E-04   6.94+11
    7.60E-04   5.45+11
    9.60E-04   7.24+11
    1.28E-03   5.44+11
    1.60E-03   5.56+11
    2.00E-03   7.29+11
    2.70E-03   5.59+11
    3.40E-03   6.77+11
    4.50E-03   4.97+11
    5.50E-03   6.39+11
    7.20E-03   5.80+11
    9.20E-03   6.50+11
    1.20E-02   5.57+11
    1.50E-02   5.73+11
    1.90E-02   7.55+11
    2.55E-02   6.69+11
    3.20E-02   5.42+11
    4.00E-02   7.76+11
    5.25E-02   7.14+11
    6.60E-02   1.00+12
    8.80E-02   7.46+11
    1.10E-01   8.20+11
    1.35E-01   6.91+11
    1.60E-01   7.37+11
    1.90E-01   6.68+11
```

```
    2.20E-01   7.25+11
    2.55E-01   7.39+11
    2.90E-01   5.88+11
    3.20E-01   7.81+11
    3.60E-01   6.58+11
    4.00E-01   6.37+11
    4.50E-01   7.09+11
    5.00E-01   6.94+11
    5.50E-01   6.58+11
    6.00E-01   7.58+11
    6.60E-01   6.99+11
    7.20E-01   7.22+11
    7.80E-01   6.77+11
    8.40E-01   8.01+11
    9.20E-01   6.31+11
    1.00E+00   1.51+12
    1.20E+00   1.31+12
    1.40E+00   1.15+12
    1.60E+00   9.96+11
    1.80E+00   8.46+11
    2.00E+00   1.07+12
    2.30E+00   9.16+11
    2.60E+00   7.28+11
    2.90E+00   7.65+11
    3.30E+00   5.55+11
    3.70E+00   4.32+11
    4.10E+00   3.49+11
    4.50E+00   3.20+11
    5.00E+00   2.22+11
    5.50E+00   1.61+11
    6.00E+00   1.62+11
    6.70E+00   8.84+10
    7.40E+00   5.62+10
    8.20E+00   2.99+10
    9.00E+00   2.75+10
    1.00E+01   1.33+10
    1.10E+01   8.02+09
    1.20E+01   1.65+09
    1.30E+01   2.22+09
    1.40E+01   6.76+08
    1.50E+01   0
    1.60E+01   0
C material card
C  AN/Iso  atom %
C From modelling hfir pager 34
C From TRIGA model Cladding material Al
```

```
m1       5010.80c 2.3945E-7 12024.80c 5.3511E-4 12025.80c 6.5030E-5  $ 6061-T6
aluminum
         12026.80c 6.8851E-5 13027.80c 5.9015E-2 14028.80c 3.2153E-4
         14029.80c 1.5771E-5 14030.80c 1.0062E-5 24050.80c 2.6872E-6
         24052.80c 4.9830E-5 24053.80c 5.5435E-6 24054.80c 1.3544E-6
         29063.80c 5.0017E-5 29065.80c 2.1628E-5
C From Michael Eades LEU Graphite Composite Fuel MCNP
C  Graphite Fuel UC-ZrC mix with 19.9% U235 with 0.640 g/cc of UC
C temp at 300 K
m2  40090.80c 0.0099844321
    40091.80c 0.0021773630
    40092.80c 0.0033281440
    40094.80c 0.0033727780
    40096.80c 0.0005433705
    6000.80c  0.1087380524
    92235.80c 0.0005074118
    92238.80c 0.0020617620
mt2 grph.18t
C from modelling hfir page 32
C Water in core region --Avg. Density = 0.98465 g/cm^3
m3  1001.66c  6.63485-02  8016.66c 3.31742-02
mt3 lwtr.60t
C comes from Triga model input for air
m4  7014.80c 0.79 8016.80c 0.21 $ air
C F1:n 1.1    $ Tally current on surface 1, the capsule inner wall
C ----------------------------------------
C Power in W/cm^3 using the tallies power point
f14:n 3 8i 12    $ Track length in cells 3-12
C multiplier from flux multiplier slides
C     atom density (a/b*cm) and material
fm14   -1.2352E4 2 (-6 -8)  $ multiplier card ( W/cm^3)
C ------------------------------------------------
C Converts to Flux at 1 MW power n/(cm^2*s)
f24:n 3 8i 12  $ Track length in cells 3-12
fm24   7.71355E16  $ multiplier card ( n/(cm^2*s))
C Neutron heating w/cm^3
f34:n 3 8i 12
fm34 7.87072E-02 2 1 -4
C Gamma Heating w/cm^3
f44:p 3 8i 12
fm44 7.87072E-02 2 -5 -6
C ------------------------------------------------
f6:n 3 8i 12  $ Track length estimate of energy deposition cell 2
f7:n 3 8i 12  $ Track length estimate of fission energy deposition cell 2
nps 1E7
```

```
HFIR capsule design
HFIR capsule design
C Cell Cards
C  Material  Density (g/cm^3)  Surfaces
1    1       -2.7              -1 2        imp:n=1               $ aluminium container
2    4       -1.029e-3          -2 3        imp:n=1               $ air gap
3    2       -3.686            -3 -11      imp:n=1  vol=.146705    $ fuels sample 1
4    2       -3.686            -3 -12 11    imp:n=1  vol=.146705    $ fuels sample 2
5    2       -3.686            -3 -13 12    imp:n=1  vol=.146705    $ fuels sample 3
6    2       -3.686            -3 -14 13    imp:n=1  vol=.146705    $ fuels sample 4
7    2       -3.686            -3 -15 14    imp:n=1  vol=.146705    $ fuels sample 5
8    2       -3.686            -3 -16 15    imp:n=1  vol=.146705    $ fuels sample 6
9    2       -3.686            -3 -17 16    imp:n=1  vol=.146705    $ fuels sample 7
10   2       -3.686            -3 -18 17    imp:n=1  vol=.146705    $ fuels sample 8
11   2       -3.686            -3 -19 18    imp:n=1  vol=.146705    $ fuels sample 9
12   2       -3.686            -3     19    imp:n=1  vol=.146705    $ fuels sample 10
13   3        0.98465           -4 1        imp:n=1               $ water around container
14   0                         4          imp:n=0               $ void

C Surface Cards
C Units are in cm
C surface cards: the dimensions and locations of these cylinders need to be modified
C Capsule dimensions, 6.50748 cm height, radius of .5549 cm with a thickness
of .23105 cm
1 RCC 0 0 -3.25374    0 0 6.50748   .5549             $ outer surface of the Capsule
2 RCC 0 0 -3.02269    0 0 6.04538   .32385             $ Inner surface of the Capsule
3 RCC 0 0 -2.77812    0 0 5.55625   .2900             $ air gap from capsule to fuel
c Added surfaces to divide Capsule into 10, .555625 cm axial segments
11  pz  -2.222495
12  pz  -1.66687
13  pz  -1.111245
14  pz  -0.555625
15  pz   0.0
16  pz   0.555625
17  pz   1.11125
18  pz   1.66687
19  pz   2.222495
4   SO   8.0
5   CZ   6.0          $ cylinder on the Z axis with radius 4.3 cm

C Create source a surface source around the target at 0 0 0
mode N
SDEF  SUR=5 dir=-1 POS=0 0 -5 RAD=6.0 EXT=d1 AXS=0 0 1 ERG=D2 $ The
Source is on the outer edge of surface 5 facing in ward
SI1 0 10
SP1 0 1
```

```
C Triga ICIT flux spectrum
#  SI2 SP2  $ the reactor source distribution
    0         0
    4.00E-08   2.50E+14
    8.00E-08   2.50E+14
    1.20E-07   2.50E+14
    1.60E-07   2.50E+14
    2.00E-07   2.50E+14
    2.40E-07   2.50E+14
    2.80E-07   2.50E+14
    3.20E-07   2.50E+14
    3.60E-07   2.50E+14
    4.00E-07   2.50E+14
    0.183      6.32E+13
    0.283      6.32E+13
    0.383      6.32E+13
    0.483      6.32E+13
    0.583      6.32E+13
    0.683      6.32E+13
    0.783      6.32E+13
    0.883      6.32E+13
    0.983      6.32E+13
    1.083      6.32E+13
    2.00E+00   6.32E+13
    3.00E+00   6.32E+13
    4.00E+00   6.32E+13
    5.00E+00   6.32E+13
    6.00E+00   6.32E+13
    7.00E+00   6.32E+13
    8.00E+00   6.32E+13
    9.00E+00   6.32E+13
    1.00E+01   6.32E+13
    1.60E+01   0
C material card
C  AN/Iso  atom %
C From modelling hfir pager 34
C From TRIGA model Cladding material Al
m1       5010.80c 2.3945E-7 12024.80c 5.3511E-4 12025.80c 6.5030E-5  $ 6061-T6
aluminium
         12026.80c 6.8851E-5 13027.80c 5.9015E-2 14028.80c 3.2153E-4
         14029.80c 1.5771E-5 14030.80c 1.0062E-5 24050.80c 2.6872E-6
         24052.80c 4.9830E-5 24053.80c 5.5435E-6 24054.80c 1.3544E-6
         29063.80c 5.0017E-5 29065.80c 2.1628E-5
C From Michael Eades LEU Graphite Composite Fuel MCNP
C  Graphite Fuel UC-ZrC mix with 19.9% U235 with 0.640 g/cc of UC
C Temp at 300 K
```

```
m2   40090.80c 0.0099844321
     40091.80c 0.0021773630
     40092.80c 0.0033281440
     40094.80c 0.0033727780
     40096.80c 0.0005433705
     6000.80c  0.1087380524
     92235.80c 0.0005074118
     92238.80c 0.0020617620
mt2 grph.18t
C from modelling hfir page 32
C Water in core region --Avg. Density = 0.98465 g/cm^3
m3  1001.66c  6.63485-02  8016.66c 3.31742-02
mt3 lwtr.60t
C comes from Triga model input for air
m4  7014.80c 0.79 8016.80c 0.21 $ air
C F1:n 1.1  $ Tally current on surface 1, the capsule inner wall
C ----------------------------------------
C Power in W/cm^3 using the tallies power point
f14:n 3 8i 12    $ Track length in cells 3-12
C multiplier from flux multiplier slides
C     atom density (a/b*cm) and material
fm14  -1.04992E6 2 (-6 -8)  $ multiplier card ( W/cm^3)
C --------------------------------------------------
C Converts to Flux at 1 MW power n/(cm^2*s)
f24:n 3 8i 12  $ Track length in cells 3-12
fm24   6.55651E18  $ multiplier card at 85 MW ( n/(cm^2*s)
C Neutron heating w/cm^3
f34:n 3 8i 12
fm34 7.87072E-02 2 1 -4
C Gamma Heating w/cm^3
f44:p 3 8i 12
fm44 7.87072E-02 2 -5 -6
C --------------------------------------------------
f16:n 3 8i 12  $ Track length estimate of energy deposition cell 2
f7:n 3 8i 12  $ Track length estimate of fission energy deposition cell 2
nps 1E7


ATR capsule design
C Cell Cards
C  Material  Density (g/cm^3)  Surfaces
1    1      -7.86          -1 2       imp:n=1            $ SS 304 container
2    4       0.0422         -2 3       imp:n=1             $ zirconium clad
3    2      -3.686         -3 -11      imp:n=1  vol=.825573    $ fuels sample 1
4    2      -3.686         -3 -12 11   imp:n=1  vol=.825573    $ fuels sample 2
5    2      -3.686         -3 -13 12   imp:n=1  vol=.825573    $ fuels sample 3
6    2      -3.686         -3 -14 13   imp:n=1  vol=.825573    $ fuels sample 4
```

```
7   2      -3.686          -3 -15 14    imp:n=1  vol=.825573    $ fuels sample 5
8   2      -3.686          -3 -16 15    imp:n=1  vol=.825573    $ fuels sample 6
9   2      -3.686          -3 -17 16    imp:n=1  vol=.825573    $ fuels sample 7
10  2      -3.686          -3 -18 17    imp:n=1  vol=.825573    $ fuels sample 8
11  2      -3.686          -3 -19 18    imp:n=1  vol=.825573    $ fuels sample 9
12  2      -3.686          -3     19    imp:n=1  vol=.825573    $ fuels sample 10
13  3       0.98465         -4 1        imp:n=1                 $ water around container
14  0                     4          imp:n=0              $ void

C Surface Cards
C Units are in cm
C surface cards: the dimensions and locations of these cylinders need to be modified
C Capsule dimensions, 24.3687 cm height, radius of .58801 cm
1 RCC 0 0 -12.1843    0 0 24.3687   .58801            $ outer surface of the Capsule SS
304
2 RCC 0 0 -7.69112    0 0 15.3822   .48641            $ Inner surface of the Capsule
Zirc
3 RCC 0 0 -7.62000    0 0 15.2400   .41529            $ From inner surface of capsule
to fuel
c Added surfaces to divide Capsule into 10, 1.524 cm axial segments
11  pz  -6.096
12  pz  -4.572
13  pz  -3.048
14  pz  -1.524
15  pz  0.0
16  pz  1.524
17  pz  3.048
18  pz  4.572
19  pz  6.096
4   SO   13.0                                  $ area around capsule water
5   CZ   6.0          $ cylinder on the Z axis with radius 4.3 cm

C Create source a surface source around the target at 0 0 0
mode N
SDEF  SUR=5 dir=-1 POS=0 0 -8 RAD=6.0 EXT=d1 AXS=0 0 1 ERG=D2 $ The
Source is on the outer edge of surface 5 facing in ward
SI1 0 16
SP1 0 1
#  SI2 SP2  $ the reactor source distribution
    0         0
    6.25E-08      3.17E+13
    1.25E-07      3.17E+13
    1.88E-07      3.17E+13
    2.50E-07      3.17E+13
    3.13E-07      3.17E+13
    3.75E-07      3.17E+13
```

```
    4.38E-07     3.17E+13
    5.00E-07     3.17E+13
    5.63E-07     3.17E+13
    6.25E-07     3.17E+13
    1.0E+0       9.39E+12
    2.0E+0       9.39E+12
    3.0E+0       9.39E+12
    4.0E+0       9.39E+12
    5.0E+0       9.39E+12
    6.0E+0       9.39E+12
    7.0E+0       9.39E+12
    8.0E+0       9.39E+12
    9.0E+0       9.39E+12
    1.0E+01      9.39E+12
    2.0E+01   0
C material card
C  AN/Iso  atom %
C From modelling hfir pager 34
C From TRIGA model Cladding material SS 304
m1       6000.81c 0.00031519 24050.81c 7.8200E-4 24052.81c 1.4501E-2 $ SS 304
Clad
         24053.81c 1.6130E-3 24054.81c 3.9400E-4 26054.81c 3.5540E-3
         26056.81c 5.5110E-2 26057.81c 1.2570E-3 26058.81c 1.6600E-4
         28058.81c 5.5580E-3 28060.81c 2.0700E-3 28061.81c 8.8500E-5
         28062.81c 2.7800E-4 28064.81c 6.8500E-5
C From Michael Eades LEU Graphite Composite Fuel MCNP
C  Graphite Fuel UC-ZrC mix with 19.9% U235 with 0.640 g/cc of UC
C temp at 600 K
m2   40090.81c 0.0099844321
     40091.81c 0.0021773630
     40092.81c 0.0033281440
     40094.81c 0.0033727780
     40096.81c 0.0005433705
     6000.81c  0.1087380524
     92235.81c 0.0005074118
     92238.81c 0.0020617620
mt2 grph.18t
C from modelling hfir page 32
C Water in core region --Avg. Density = 0.98465 g/cm^3
m3  1001.66c  6.63485-02  8016.66c 3.31742-02
mt3 lwtr.60t
C comes from Triga model zirconium
m4       40090.81c .5219 40091.81c .1125 40092.81c .1702 $ zirconium
         40094.81c .1688 40096.81c .0266
C F1:n 1.1  $ Tally current on surface 1, the capsule inner wall
C ----------------------------------------
```

```
C Power in W/cm^3 using the tallies power point
f14:n 3 8i 12    $ Track length in cells 3-12
C multiplier from flux multiplier slides
C     atom density (a/b*cm) and material
fm14  -2.2717E5 2 (-6 -8)  $ multiplier card ( W/cm^3)
C ---------------------------------------------------
C Converts to Flux at 1 MW power n/(cm^2*s)
f24:n 3 8i 12  $ Track length in cells 3-12
fm24   1.69698E18  $ multiplier card at 22 MW ( n/(cm^2*s))
C Neutron heating w/cm^3
f34:n 3 8i 12
fm34 7.87072E-02 2 1 -4
C Gamma Heating w/cm^3
f44:p 3 8i 12
fm44 7.87072E-02 2 -5 -6
C ---------------------------------------------------
f16:n 3 8i 12  $ Track length estimate of energy deposition cell 2
f7:n 3 8i 12  $ Track length estimate of fission energy deposition cell 2
nps 1E7
```